Construction of metal-pincer complexes from a hydrophilic-hydrophobic library

A.D. Filippov

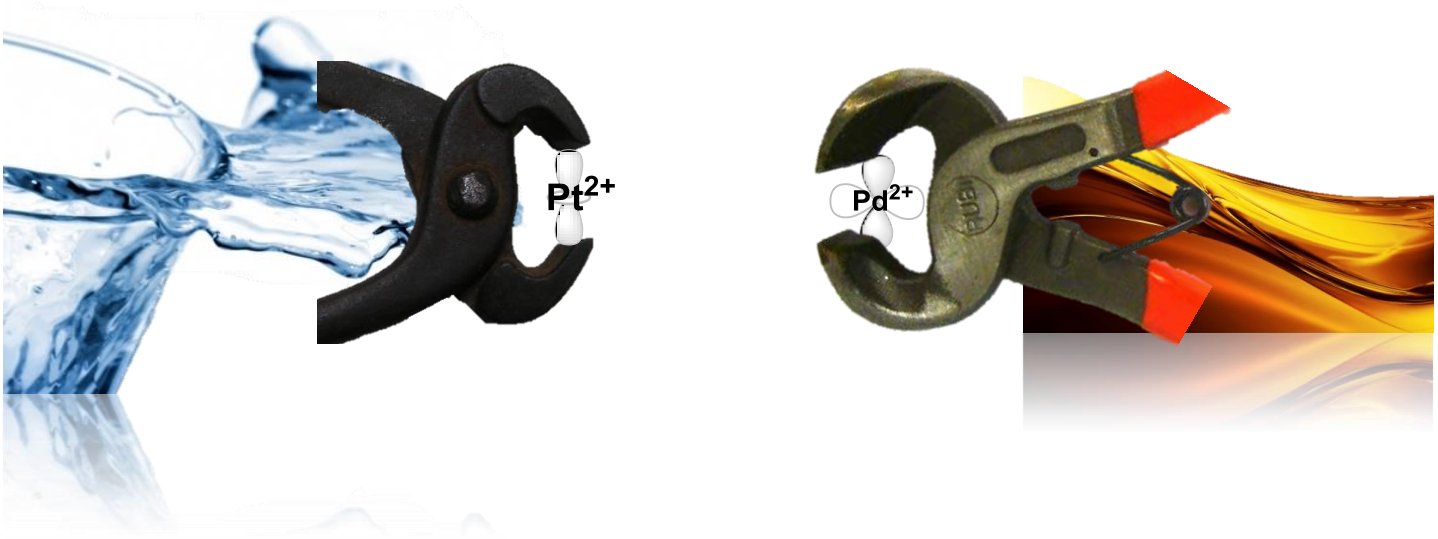

Construction of metal-pincer complexes from a hydrophilic-hydrophobic library

An MSc thesis project

November 2014 – April 2015
to be credited with 24 ECTS
for course ORC-80424

Aljosha D. Filippov
Registered as number 920212240090

supervised by
Dr. Ir. Maarten M. J. Smulders
Dr. Fátima García Melo

examined by
Dr. Ir. Maarten M. J. Smulders
Dr. Fátima García Melo
Dr. Ing. Tom Wennekes

at the Laboratory of Organic Chemistry,
Responsive Supramolecular Polymers Group
Department of Agrotechnology and Food Sciences
Wageningen University and Research Centre

Contents

1. Introduction

In chemistry, a dynamic system is one in which bonds associate and dissociate on a similar timescale. In such systems, only configurations that are significantly lower in energy than the others will populate the system.[1] Bonds that drive these dynamic assemblies often rely on non-covalent (weak) interactions, such as hydrophobic interactions, Van der Waals interactions, hydrogen bonds, π–π stacking and metal-ligand coordination.[2] Assembly of multiple molecules using these bonds is called supramolecular self-assembly, and it is the principle that governs fundamental mechanisms in biology such as protein folding and nucleosome organization.[3] Certain covalent bonds are reversible as well,[4] such as boron-oxygen[5] and imine[6] bonds. In dynamic covalent chemistry, such bonds are employed to recover a one (or few) out of many possible products from covalent, equilibrium-driven reactions.[1,4,6,7] Assemblies that are constructed from dynamic building blocks are intrinsically responsive to environmental conditions, such as temperature and concentrations of electrolytes. Dynamically assembled assemblies have found use in applications were responsive behavior is desirable, such as biosensing[8], bioimaging[9] and drug delivery.[10]

Metal ions of the *d*-block are versatile building blocks for chemical structures that form supramolecular assemblies.[11] They are used to bond ligands in a highly directional, responsive fashion,[12] as well as to imbue organic materials with desirable properties, such as catalytic activity[13] and luminescence.[14] By outfitting organic molecules with features that drive association orthogonally to metal-ligand binding, the functionality of metal ions can be assimilated into supramolecular, responsive materials. This allows construction of metal-organic structures on the mesoscale, such as ultrasound-responsive micelles from two copolymers terminated with terpyridine and coordinated by Cu(II),[15] bilayered sheets from an amphiphilic two-ligand Pt(II)-complex that transforms into micelles when heated[16] (Figure 1a), and self-healing, phosphorescent gels formed from Pt(II)-ligand complexes associated through metallophilic Pt···Pt interactions and π–π stacking,[17,18] or even cross-linked with small amounts of a di-Pt(II) linker.[19] In terms of functionality, most accomplished are perhaps several examples of Pt(II)-ligand systems that associate in cells to form highly phosphorescent assemblies with high quantum yields and long-lived excited states (Figure 1b).[9]

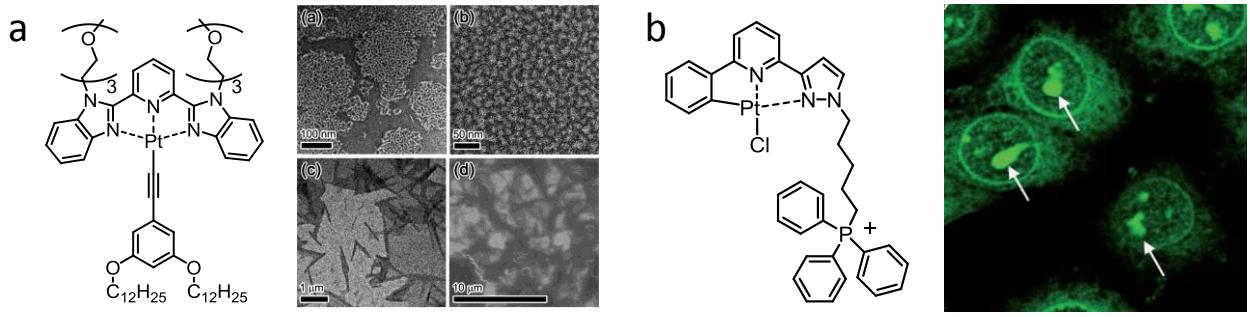

Figure 1: Responsive, self-assembled materials from Pt(II)-ligand complexes, **(a)** a water-soluble, amphiphilic Pt-complex assembles into bilayered sheets at room temperature (lowermost TEM images) that transforms into micelles when heated (uppermost TEM images), adapted from ref. [16] **(b)** Pt(II)-ligand complex that assembles in cells to form phosphorescent nanostructures useful for bioimaging (micrograph to the right), adapted from ref. [20].

The imine bond(–C=N–) is known to coordinate to metal ions, as well as to form from and dissociate into the corresponding amine and aldehyde dynamically, whilst still being covalent. These features were previously showcased in the synthesis of tetrahedral bis(diimine)-copper(I) complexes by the group of Nitschke[7], shown in Figure 2. Initially, two diimines are mixed. However, due to imines being in equilibrium with their amine and aldehyde constituents, these two diimines are in equilibrium with a third, "mixed" diimine. Addition of copper results in an even larger variety of copper complexes to either one or two diimine molecules, which do not have to be identical. However, because the system is dynamic, only the two most stable copper(I)-diimine complexes end up as products over time. Thus, metal-templated imine motives are useful in dynamic covalent synthesis.

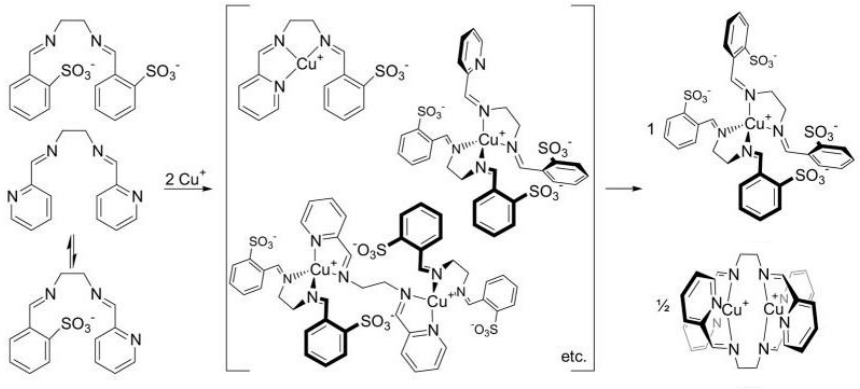

Figure 2: Copper(I)-bis(diimine) complexes in a dynamic process that produces two specific products out of the many possible ones. Adapted from Nitschke and co-workers.[7]

Another class of a metal-templated imines are 2,6-diiminophenylpyridine tridentate (pincer) ligands with Pd(II) as a template.[21] They have a square planar geometry, which strongly promotes stacking of the extended π-system and the Pt orbitals that are not involved in ligand chelation.[22–24] Nonetheless, the aggregation capability of square planar diiminobenzylpyridine-metal complexes has not yet been investigated. Therefore, of interest is the design of a square-planar Pt(II)/Pd(II)-diiminophenylpyridine architecture in which the chemical groups that determine the solvent-ligand interactions are coupled *via* an imine bond. This allows to outfit the metal-pincer complex with groups that are hydrophobic or hydrophilic in equilibrium-controlled reactions, which could allow formation of aggregates of which the morphology would be dynamically tunable: the groups attached *via* the imine bond can be exchanged in an equilibrium reaction when the exchanged imine is more stable.

1.1. Objective

In this Thesis, the synthesis of Pt(II) and Pd(II)-complexes of 2,6-diiminobenzylpyridines from a set of hydrophilic and hydrophobic building blocks is explored. Pt(II) and Pd(II) were chosen as metal ions because of their square planar coordination with tridendate ligands. In addition, the former ion displays well-known aggregation-induced luminescence, which would be a facile probe to assess metal-ligand complexation. Figure 3 shows the synthetic route towards these complexes starting from the synthesis of pincer ligands from the corresponding anilines and 2,6-pyridinedicarbaldehydes. By synthesizing hydrophilic or hydrophobic analogues of these building blocks (R_1 and R_2 in Figure 3), diimino pincers with hydrophobic, hydrophilic and amphiphilic character can be made. Finally, after metalation, coordination of the metal-pincer complex to a phenylisocyanide or pyridine derivative provides a final opportunity to control the character of the complex. Such monovalent Pt-ligands are referred to as ancillary ligands.

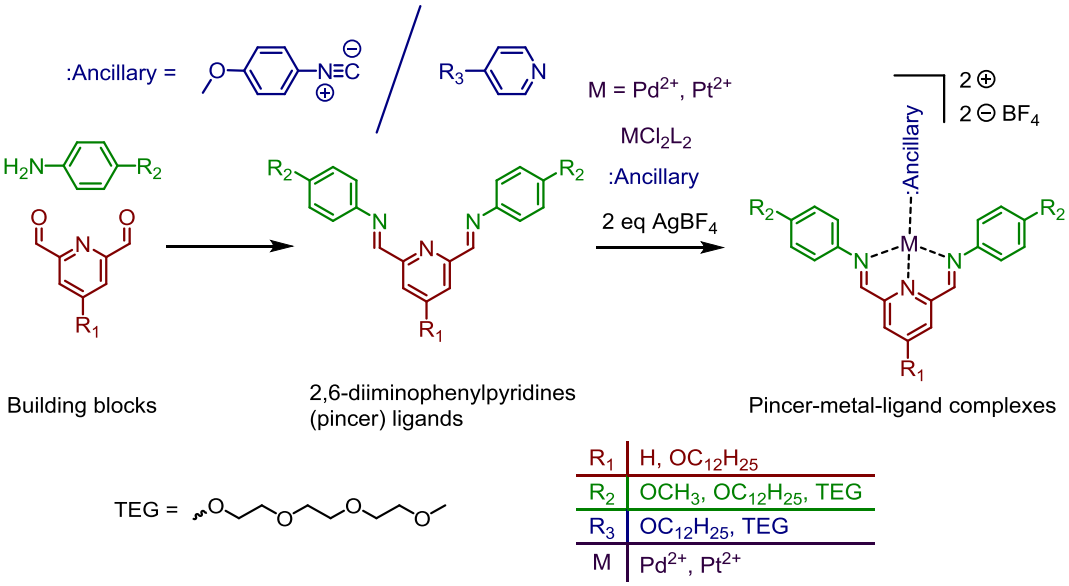

Figure 3: Synthesis of pincer-metal-ancillary complexes from corresponding pincer ligands, ancillary ligands and a metal salt. The ligands themselves are synthesized in one step from building blocks.

2. Results & Discussion

Herein, complexation of Pt^{2+} and Pd^{2+} ions with 2,6-diiminophenylpyridine pincer ligands is reported. These ligands were synthesized from a set of hydrophilic and hydrophobic components to control their interactions with solvents, and therefore their solubility and aggregation potential. Additionally, the interaction with pyridines and methoxyphenylisocyanide in solution is studied. This Section is split so that Section 2.1 focuses on the synthesis of the building blocks, Section 2.2 describes the synthesis of the pincer ligands and their Pt/Pd complexes. Furthermore, Section 2.3 presents our findings in attempts to coordinate pyridines and methoxyphenylisocyanide to the complexes.

2.1.Synthesis of building blocks

The molecules that can act as monovalent ligands to metal-pincer complexes, as well as the molecules from which the pincer ligand is generated are referred to as building blocks (see Figure 3). In this Section, synthesis of 4-dodecyloxy 2,6-pyridinedicarboxaldehyde and 4-derivatized aniline building blocks that can generate the tridentate pincer are described first, followed by synthesis of the monovalent pyridine and 4-methoxyphenylisocyanide ligands.

2.1.1. Synthesis of 4-dodecyl-2,6-pyridinedicarboxaldehyde

Figure 4 shows the synthesis of a hydrophobic pyridinedicarboxaldehyde building block, adapted from a work by Busto and co-workers.[25] Chelidamic acid (4-hydroxy-2,6-pyridinedicarboxylic acid) is the initial precursor, and the transformation into the building block occurs over the course of four chemical reactions. Fischer esterification with ethanol on the carboxylic acid moieties yielded diester **1**, which was purified by extraction to yield an off-white sticky solid in 61% yield. A previous report on synthesis of **1** from our laboratory notes a significant degree of substitution of the phenol to form the 4-ethoxy derivative and incomplete conversion to the monoethyl ester. In contrast, the material obtained here was pure enough to avoid column chromatography.

The diester **1** was *O*-alkylated by a nucleophilic substitution reaction with dodecyl bromide in DMF in presence of a base. Thin layer chromatography on silica showed that the transformation gave at least three highly mobile by-products. An attempt to extract **2** from the evaporated reaction mixture in ethyl acetate/ice water resulted in a highly stable emulsion which did not break up even after standing for a week. This is attributed to traces of DMF in the reaction mixture that resisted evaporation. The crude alkylated product was recovered by dehydration of the emulsion by $MgSO_4$ and purified by column chromatography over silica slurry in DCM to give pure 4-dodeoxy-2,6-pyridine-diethyl ester **2** in 36% yield. The work-up should be improved by avoiding emulsification during extractive work-up, while further optimization of reaction conditions could lower the extent of by-product formation.

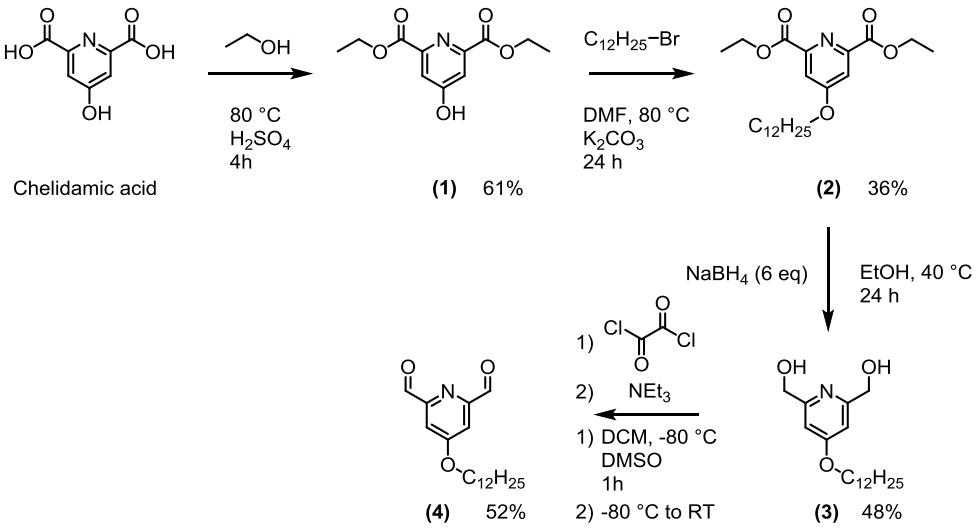

Figure 4: Synthesis of 4-dodecyloxy-2,6-pyridinedicarbaldehyde (**4**) from chelidamic acid.

As shown in Figure 4, compound **2** was reduced to the corresponding diol **3** by action of a hydride donor on the two carboxylic carbon atoms. This was achieved by reaction with six equivalents of sodium borohydride in absolute ethanol at 40 °C. Thin layer chromatography on silica using MeOH:DCM (95:5) as eluent showed a spot at the baseline (R_f = 0) along with the mobile product (R_f = 0.52) upon complete conversion of the starting material. Shaking a solution of the crude in ethyl acetate with brine yielded an emulsion that only broke up after standing for one day. The kinetic stability of the emulsion is attributed to the amphiphilic nature of compound **3**, which has a strongly apolar dodecyl chain along with a polar 2,6-dihydroxyethylpyridine head group (Figure 5). Additionally, when water was evaporated from a crude mixture of **3**, the solution foamed intensely. Nonetheless, the time-consuming extraction yielded compound **3** in 48% yield, pure enough to avoid further purification. Because product and by-product have such different retentions on silica, filtration to remove sodium salts followed by flash chromatography would be a better purification strategy.

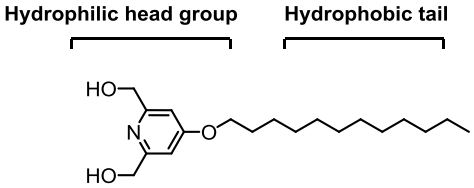

Figure 5: Structure of 4-dodeoxy-2,6-dihydroxyethylpyridine with emphasis on its amphiphilic character.

Finally, the dicarbaldehyde building block was generated through Swern oxidation of the two hydroxy moieties by the action of 2.5 equivalents of thionyl chloride and 5 equivalents of DMSO in DCM at -80 °C, followed by quenching with NEt_3. The DCM solution of crude **4** was washed seven times with bleach to remove any dimethyl sulfide that is generated as a by-product, and next with water to remove the bleach. Thin layer chromatography on silica in heptane:ethyl acetate (4:1) showed seven spots with R_f

between 0.0 and 0.64. After column chromatography on silica in an eluent gradient from heptane to heptane:ethyl acetate (6:1), pure 4-dodeoxy-2,6-pyridinedicarboxaldehyde was isolated in 52% yield. The product could easily be followed on silica, as it had a bright pink colour on the column. Figure 6 shows the ^{1}H-NMR spectrum of **4** in deuterated chloroform.

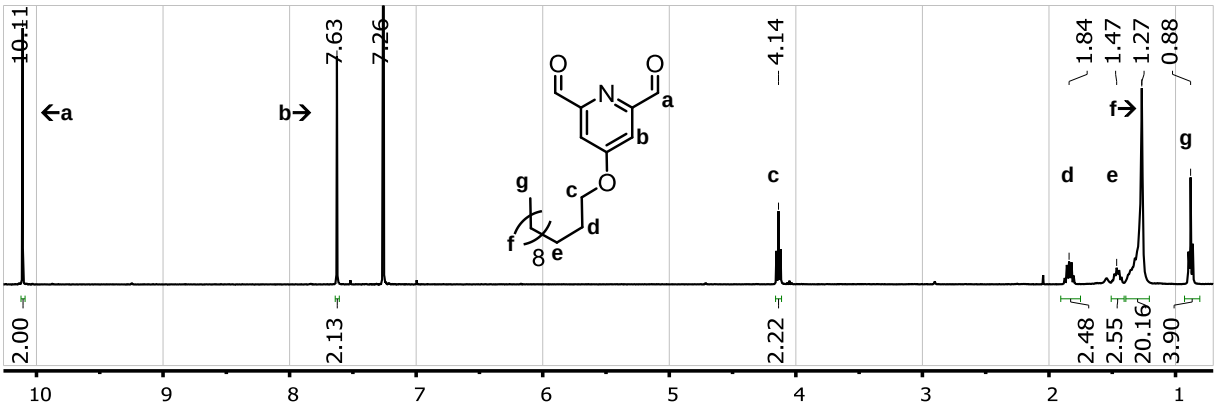

Figure 6: ^{1}H-NMR ($CDCl_3$, 400 MHz) spectrum of dodecyloxy-functionalized 2,6-pyridine dicarboxaldehyde **4** in deuterated chloroform.

The overall yield upon a start from the chelidamic acid precursor to the dialdehyl building block **4** is just above 5%. The most significant losses were due to emulsification in extraction of **2** and due to by-product formation during formation of **4**. While the route should be optimized in further attempts, the amount of material (0.8 g) was satisfactory for further experiments. In the diimination reaction (Section 2.2.1), **4** reacts with two equivalents of an aniline. In the next Section, results from synthesis of two such anilines are presented.

2.1.2. Syntheses of 4-derivatized anilines

Synthesis of two 4-substituted anilines, shown in Figure 7, was pursued: A hydrophobic aniline (**8**) that carried a dodecyl chain was synthesized, along with a hydrophilic aniline (**10**) with a methoxytri(ethylene glycol) chain.

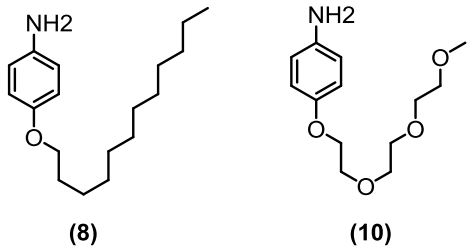

Figure 7: Hydrophobic 4-dodecyloxy-aniline **8** and hydrophilic 4-methoxytri(ethylene glycol)-aniline **10**.

2.1.2.1.Synthesis of hydrophobic 4-dodecyloxy-aniline

As shown in Figure 8, synthesis of 4-dodeoxyaniline was achieved in three steps, starting from *N*-boc protected 4-aminophenol. The alkylated *N*-boc-aniline precursor (**5**) was isolated in 80% yield after chromatography over silica in a gradient of heptane to heptane:ethyl acetate 1:1. Next, the *N*-boc protecting group was removed by the action of TFA in DCM to form the trifluoroacetate salt of **6**.

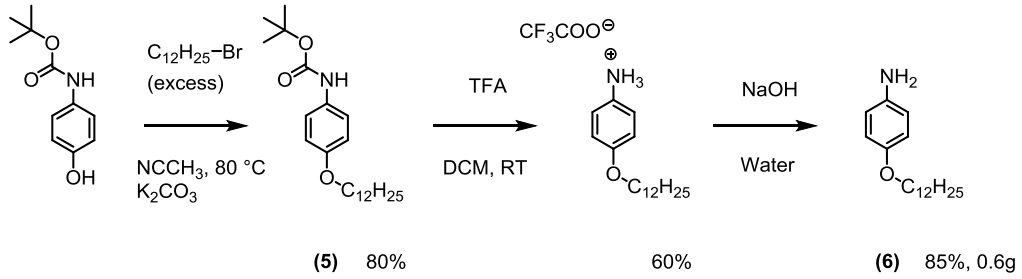

Figure 8: Synthesis of 4-dodeoxyaniline from 4-*N*-boc-aniline in three steps.

The salt was insoluble in most organic solvents, but dissolved in mixtures of MeOH and DCM (equal volumes) and in DMSO. Additionally, for a salt it is very mobile on silica with R_f-values of 0.19 and 0.69 in petroleum ether:ethyl acetate (4:1) and 5% DCM in MeOH, respectively. This seems to stem from the low affinity of the trifluoromethyl group for polar phases. The salt was successfully purified by chromatography on silica in a gradient of DCM:MeOH from 100:2 to 100:5 and isolated in 85% yield.

The amine of 4-dodeoxyaniline trifluoroacetate salt is protonated and therefore non-nucleophilic. In fact, an attempt to use this salt in an imination reaction resulted in no reaction (data not shown). The aniline was liberated by dissolving the trifluoroacetate salt in DCM:MeOH 9:1 and shaking it with aqueous NaOH. After the organic phase was dried over $MgSO_4$ and concentrated under reduced pressure, **6** was recovered in 85% yield.

2.1.2.2. Synthesis of hydrophobic and hydrophilic 4-derivatized anilines

As shown in Figure 9, a nearly identical route was attempted for the synthesis of hydrophilic 4-methoxytri(ethylene glycol)-aniline, safe for the use of a toluylsulfonate TEG-donor instead of the corresponding bromide. Toluylsulfonate **7** was prepared by stirring 4-toluenesulfonate chloride with tri(ethylene glycol) methyl ether in a suspension of KOH in DCM, and purified by washing the reaction mixture with water, $NaHCO_3$ and brine. In early attempts to synthesize aniline **10** as illustrated in Figure 9, an excess of **7** was used. During purification it turned out that both intermediate **8** and the trifluoroacetate salt **9** co-eluted with unreacted **7** under a large variety of chromatographic conditions, such as different stationary phases (silica, alumina and reversed phase silica) with a variety of common eluents (DCM, mixtures of ethyl acetate/petroleum ether, DCM/MeOH and toluene).

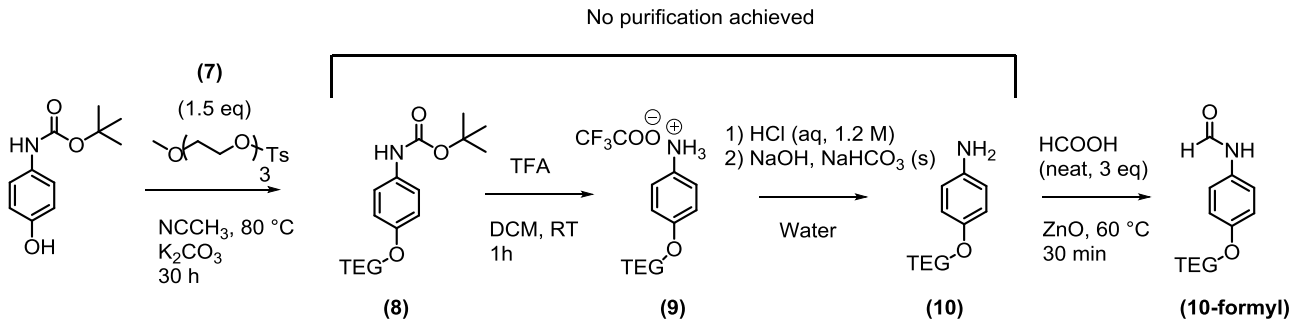

Figure 9: Unsuccessful synthesis of 4-TEG aniline **10** and successful formation of the corresponding formanilide **10-formyl**.

In an another attempt to purify the trifluoroacetate salt from leftover toluenesulfonate **7**, it was successfully converted into the hydrochloride salt by shaking it in a 15% MeOH in DCM solution with 1.2 M aqueous hydrochloric acid. The resulting aqueous solution of **9** was then neutralized by adding solid NaOH and $NaHCO_3$ until saturation. The organic content was subsequently extracted into a mixture of 10% of MeOH in DCM. This resulted in disappearance of **7** and partial degradation of product **10** into a by-product. ESI-MS suggested that the new by-product was *N*-, *O*-dimethoxy(triethylene glycol)-aniline, and thin layer chromatography showed that it co-eluted with **10** on silica in mixtures of DCM and MeOH. Thus, an excess of **7** must be avoided in the first step, due to its similar chromatographic retention to intermediates **8** and **9**, and due to its reactivity in basic workup towards **10**.

On a side note, removal of the disubstituted product was achieved by reaction of the excess of the crude **10** with formic acid in the presence of zinc oxide to generate the formanilide **10-formyl**, which was successfully isolated by washing a solution of the crude in DCM with 1M of aqueous hydrochloric acid, aqueous sodium carbonate and water. This formaldehyde can be used as a substrate for the generation of the corresponding isocyanide,[26] as described for the analogous structure *N*-formyl-4-methoxyaniline in Section 2.1.3.

2.1.2.3. 4-Methoxy(triethylene glycol)-aniline: the importance of stoichiometry

A successful synthesis of 4-methoxytri(ethylene glycol) was only achieved after the first step was changed to use a small excess of the *N*-boc precursor instead of an excess of **7**, as done in initial attempts (Figure 9). This updated route is shown in Figure 10. In all steps, all by-products and reactants could be removed by extraction. Interestingly, the trifluoroacetate salt **9** does not crystallize, but rather is an ionic liquid.

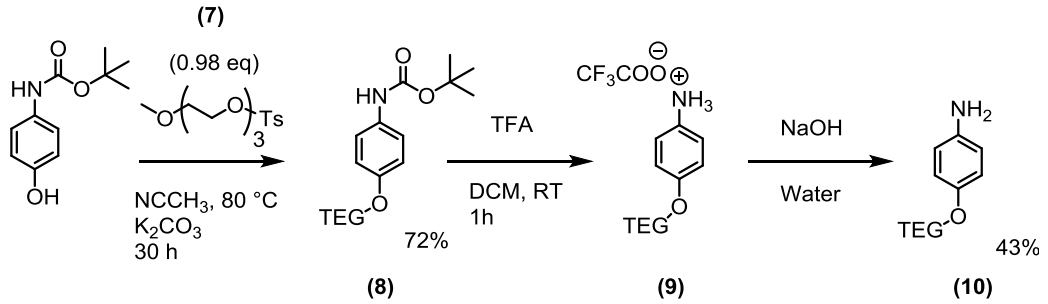

Figure 10: Synthesis of 4-methoxytri(ethylene glycol)-aniline (**10**) from *N*-boc-4-aminophenol with methoxy(triethylene glycol) tosylate (**7**).

Trifluoroacetate salt **9** is easily distinguished from liberated aniline **10** by the chemical shift of the amine peak in NMR spectroscopy, as shown in Figure 11. In the salt, the amine peak is more than 3 ppm broad and is shifted downfield as to 9-12 ppm. The free aniline has a relatively sharp amine peak in the expected region, around 3.5 ppm. Additionally, the two aromatic doublets shift closer to each other in the free aniline due to the more similar electron donating effects of the ether and amine group.

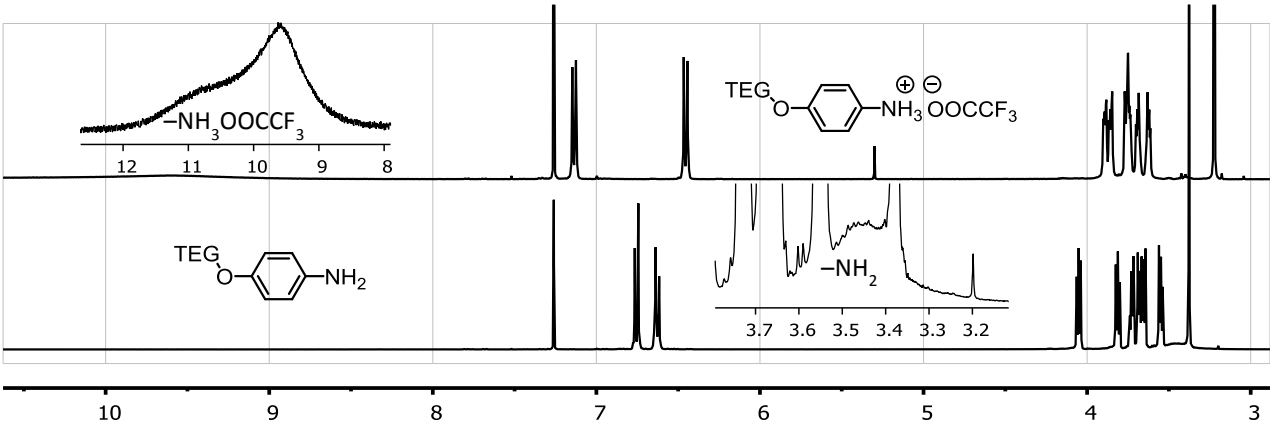

Figure 11: ^{1}H-NMR ($CDCl_3$, 400 MHz) of (top) trifluoroacetate salt **9** and (bottom) the corresponding liberated aniline. The insets are magnifications at the positions of the ammonium trifluoroacetate (top) and amine peak (bottom).

2.1.3. Synthesis of monovalent ligands

Upon dehydration, two equivalents of an aniline and one equivalent of an 2,6-pyridinedicarboxaldehyde form an diiminophenylpyridine compound that is a trivalent ligand for transition metal ions. A second ligand can then be introduced to complete the square planar coordination geometry. Previously in our group, 4-methoxy(triethylene glycol) pyridine was synthesized. Here, we describe synthesis of 4-dodeoxypyridine and 4-methoxyphenylisocyanide that could serve as monovalent ligands.

Figure 9 shows a one-step route towards the 4-substituted dodecyloxypyridine **11** by aromatic nucleophilic substitution of chlorine on the pyridine ring.[27] Thin layer chromatography on crude **11** showed a mixture of the substituted pyridine, dodecyl alcohol and one unknown by-product. The crude

solid was distilled on a short-path apparatus (200 °C, 14 mbar). The volatile fraction was predominantly dodecyl alcohol, while the non-volatile fraction was a nearly pure product. While chromatography in 5% of MeOH in DCM and in pure DCM resulted in partial and no separation, respectively, **11** was isolated by chromatography in a gradient from heptane:DCM (4:1) to DCM to MeOH:DCM (1:9).

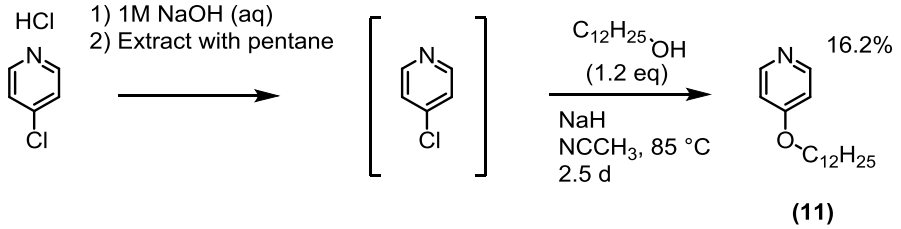

Figure 12: Synthesis of 4-dodeoxypyridine (**11**) from 4-chloropyridine hydrochlorate.

Another class of monovalent ligands that are reported to associate with transition metal-ligand complexes are isocyanides,[28] and 4-methoxyphenylisocyanide was prepared as a model to assess the feasibility of isocyanide synthesis and association to metal-diiminophenylpyridine complexes. Figure 13 illustrates the route to obtain 4-methoxyphenylisocyanide (**13**).

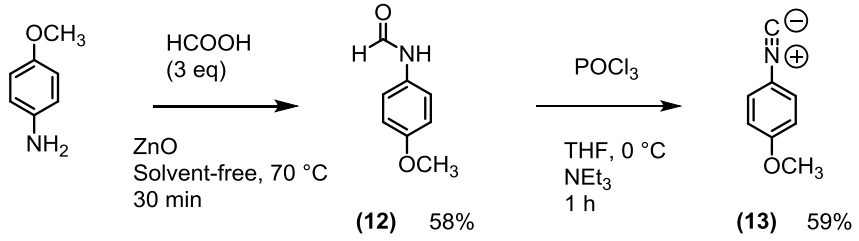

Figure 13: Synthesis of 4-methoxyisocyanide (**13**) from 4-methoxyaniline in two steps.

Formanilide **12** was obtained via a solvent-free procedure by Hosseini-Sarvari and co-workers.[29] The crude was dissolved in DCM and washed with water and aqueous sodium carbonate. While gas chromatography on the resulting product showed only one peak, the ^{1}H-NMR spectrum of solutions of **12** in deuterated methanol and chloroform reflected the presence of more than one compound. However, the rotational rigidity of the N-C amide bond[30,31] suggested that the two structures were *cis*-*trans*-isomers. Indeed, an NMR study on mono- and di- *N*-substituted formanilides showed that these compounds exist as two rotamers, whose respective concentrations are concentration- and solvent-dependent.[32] This solvent-dependency can be seen in 1H-NMR spectra of **12** in deuterated methanol and chloroform, shown in Figure 14a and b, respectively.

The positions and *J*-values of **12** correspond to spectral data from literature.[33] The well-resolved N-H resonances in the $CDCl_3$ spectrum (Figure 14b) give an estimate of the ratios between concentrations of *cis*- and *trans*-species in the mixtures. The doublet at 8.3 ppm couples to the (C=O)-H resonance (not

resolved) with J_{HNCH}=1.6 Hz, which is typical for *cis*-coupling, while the doublets at 8.49 with J_{HNCH}=11.6 Hz, which corresponds to *trans*-coupling.[32] When it is assumed that the relative positions of the two isomers in the spectrum are similar in both solvents, we can compare the ratios of the isomers, *trans*:*cis*. These are respectively 1:2 and 1:1 for CD_3OD and $CDCl_3$. Thus, both isomers have a similar stability in chloroform, while methanol prefers the *cis*-isomer more pronouncedly. The positions of the aromatic and -OCH_3 signals are hardly affected by solvent choice.

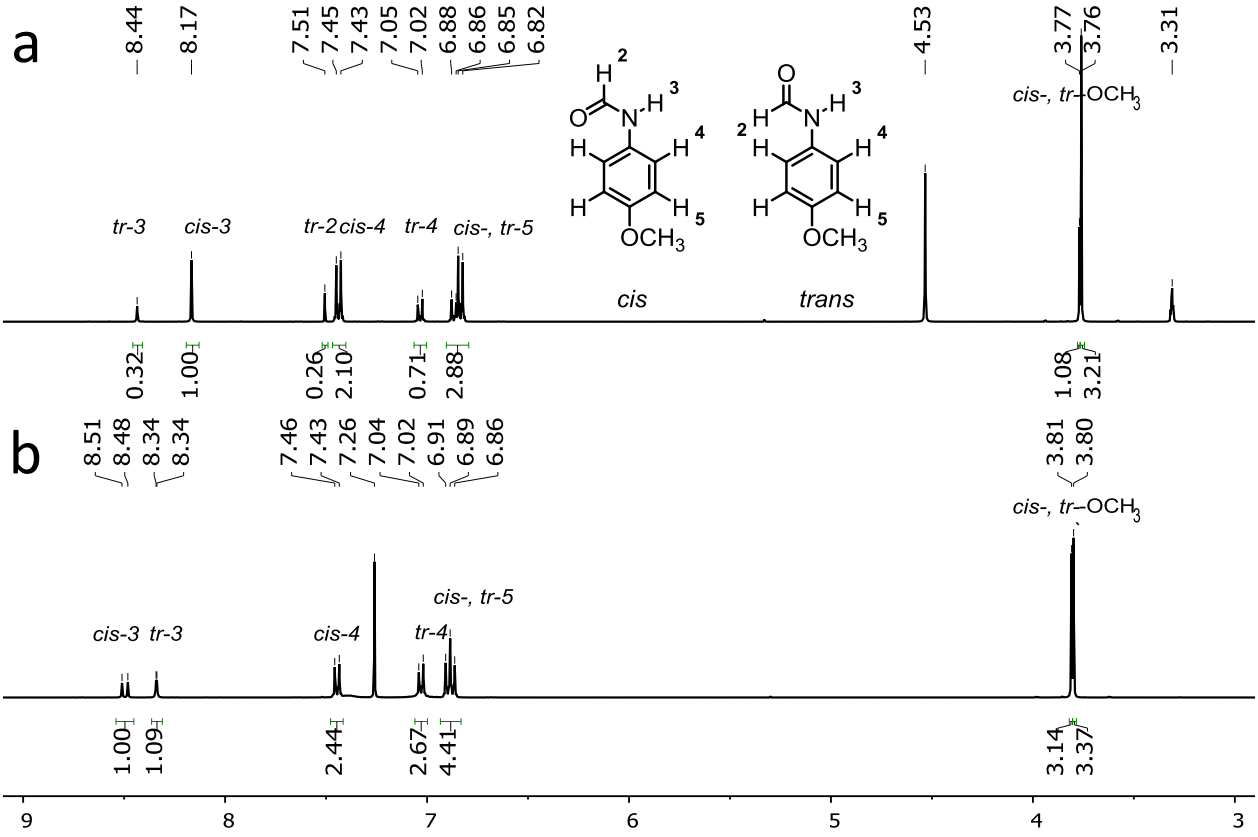

Figure 14: ^{1}H-NMR (400 MHz) of *N*-formyl-4-methoxyaniline (**12**) in **(a)** CD_3OD and **(b)** $CDCl_3$. *cis*-, *tr*- refers to a signal corresponding to respectively the *cis*- or *trans*-isomer on a proton numbered such as in the structures in the inset.

As shown in Figure 13, model isocyanide **13** was prepared by dehydration with phosphorous oxychloride in the presence of triethylamine.[34] A solution of the crude mixture in diethyl ether gave the pure isocyanide after washing with aqueous sodium carbonate and water. To generate the more hydrophilic TEG-substituted phenylisocyanide, the same procedure could be applied to *N*-formyl-4-TEG-aniline **11** in further work.

Up to now, a library of dodecyloxy- and methoxytri(ethylene glycol)-substituted building blocks has been synthesised that has the potential to form self-assembling structures in equilibrium-driven reactions. In particular, they are designed to **a)** form a 2,6-diiminophenylpyridine pincer ligand that is known to bind to metals, and in particular, platinum and **b)** associate with this pincer-metal complex. In the next

Sections, synthesis and properties of platinum- and palladium-pincer complexes based on these building blocks are discussed.

2.2. Synthesis of platinum- and palladium-2,6-diiminophenylpyridine complexes

Figure 15 illustrates the possibilities of synthesis of hydrophilic, hydrophobic and amphiphilic 2,6-diiminophenylpyridine-metal complexes with the building blocks obtained synthetically (Section 2.1) or from commercial sources. The route proceeds via the formation of the free diimine, and the subsequent insertion of a Pt^{2+} or a Pd^{2+} ion. This Section focuses first on the achieved diimino ligands and second metalation of these ligands.

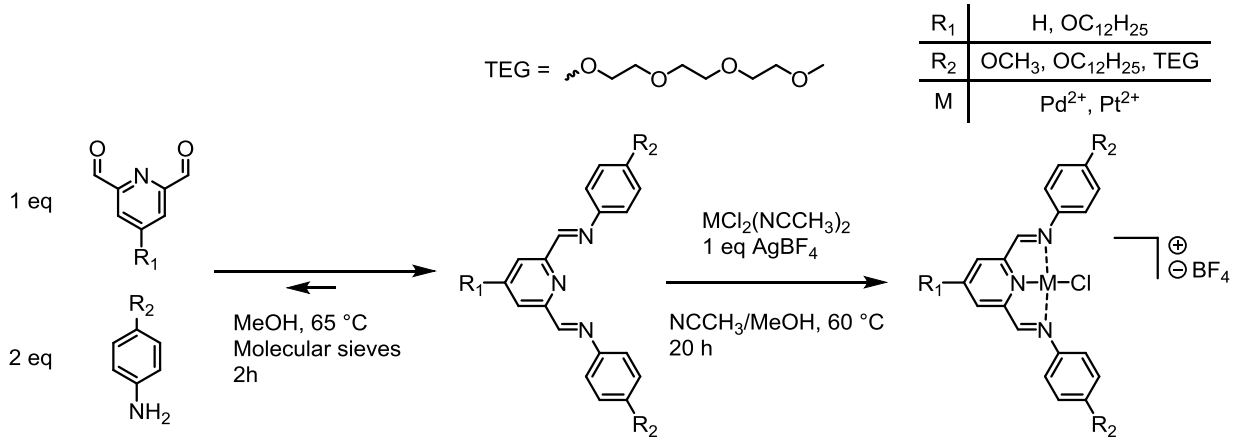

Figure 15: Assembly of pincer-metal complexes via diiminophenylpyridine ligand formation from a 2,6-pyridinedicarboxaldehyde, two equivalents of an aniline and subsequent reaction with a salt containing the metal ion.

2.2.1. Synthesis of 2,6-diiminophenylpyridine derivatives

The library of two 2,6-pyridinedicarbaldehydes (R_1=H, OCH_3) and three anilines (R_2=OCH_3, TEG, $OC_{12}H_{25}$) allows synthesis of six unique ligands, of which all but one were synthesized. A solution or dispersion of one equivalent of the dicarboxaldehyde and two equivalents of the aniline in methanol yielded the ligand after 2 hours of stirring on reflux, in the presence of molecular sieves. After reaction, DCM was poured into the mixture and the solution or dispersion was filtrated over a paper filter to remove the molecular sieves. 2,6-di(imino-4-dodecylphenyl)-4-dodeoxypyridine (diDoIPDoPy, R_1=$OC_{12}H_{25}$, R_2=$OC_{12}H_{25}$) resisted filtration and was decanted. The ligands were obtained in >95% purity. Table 1 summarizes appearance and solubility of the five 2,6-diiminophenylpyridine ligands. Figure 16 gives ^{1}H-NMR spectra of three of these ligands, along with their covalent structures with all unique protons assigned.

Table 1: Overview of synthesized 2,6-diiminophenylpyridine ligands.

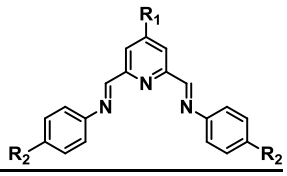

Code	R_1	R_2	Appearance	Dissolved in bulk by	Not/poorly dissolved by
diMIPPy	H	OCH_3	Yellow crystals	$CHCl_3$, DCM, DCM/MeOH	MeOH, $NCCH_3$
diDoIPPy	H	$OC_{12}H_{25}$	Yellow powder	$CHCl_3$, DCM	MeOH, DCM/MeOH
diTegIPPy	H	TEG	Yellow wax	$NCCH_3$	DCM, MeOH, $CHCl_3$, DCM/MeOH
diTegIPDoPy	$OC_{12}H_{25}$	TEG	Brown paste	Unknown	$NCCH_3$, MeOH, $CHCl_3$, DCM/MeOH
diDoIPDoPy	$OC_{12}H_{25}$	$OC_{12}H_{25}$	Red wax	Toluene, hexane	$NCCH_3$, MeOH, DCM, MeOH/DCM

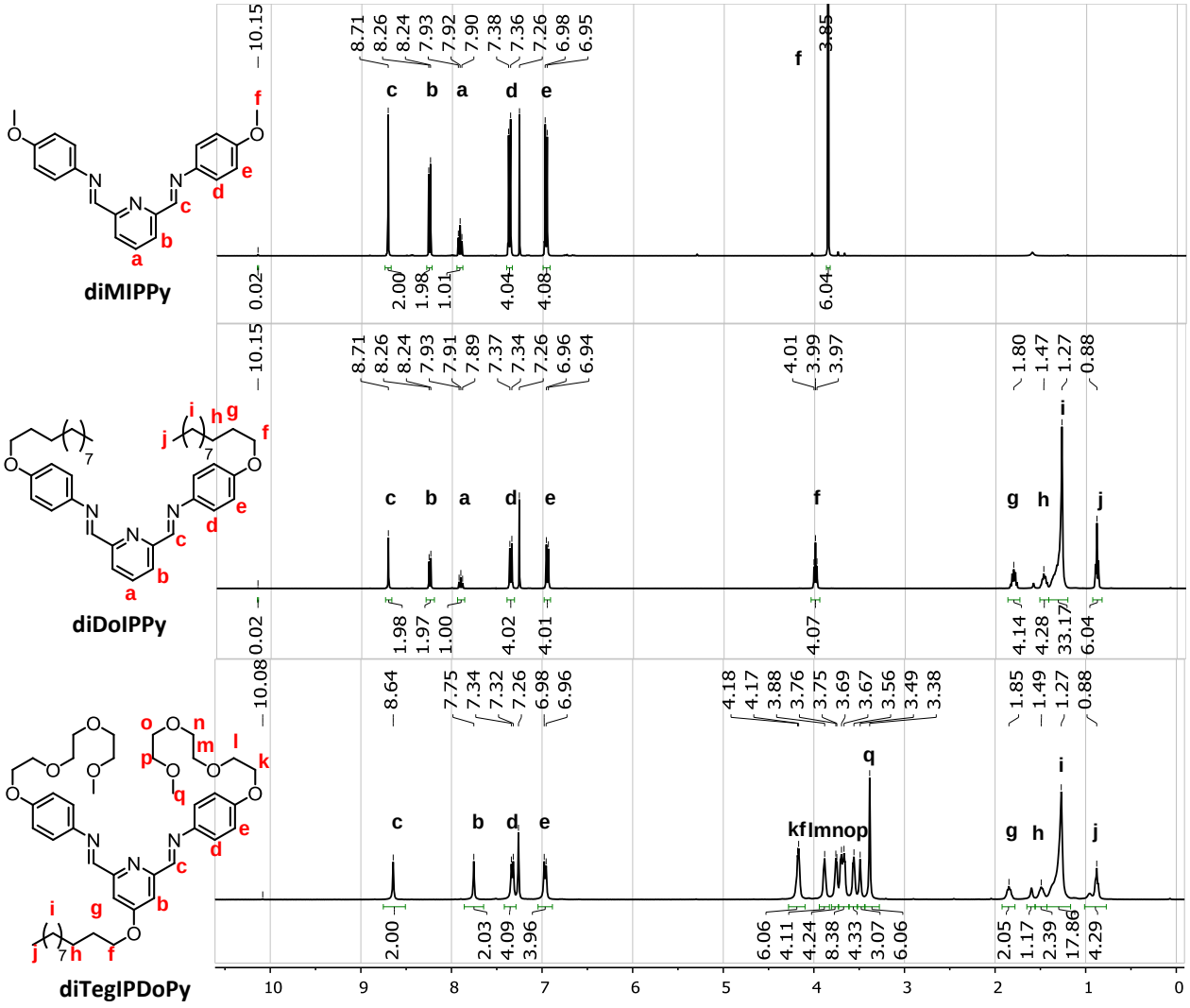

Figure 16: ^{1}H-NMR spectra ($CDCl_3$, 400 MHz) of three 2,6-diiminophenylpyridines, **(top)** diMIPPy **(middle)** diTegIPPy, and **(bottom)** diTegIpDoPy. Corresponding structures including assignment are shown left of the spectra.

In some cases, small amounts of unreacted dialdehyde or half-reacted monoaldehyde (imine formed at one carbon, aldehyde at other carbon) were observed in the NMR spectra. These impurities never contributed to more than 5%. Crystals of diMIPPy, (R_1=OCH_3, R_2=OCH_3) were washed with MeOH in an attempt to remove soluble starting materials, but this did not result in any decrease in the amount of impurities. Due to the dynamic nature of the imine bond, these ligands are always in equilibrium with the corresponding aniline and aldehyde. Therefore, they are unstable in solution in absence of desiccants. This rules out column chromatography and many other possibilities for purification, and therefore the unpurified imines of at least 95% purity (NMR) were used. These reactions gave yields around 50%, with losses in filtration due to the tendency of the imines to stick to the removed molecular sieves. Again, it is not advisable to wash them with an excess of solvent, as the imines hydrolyse at least partially in the absence of desiccants.

Table 1 shows that the solubility of the complexes in MeOH, DCM and their mixtures decreases upon attachment of TEG or dodecyloxy substituents. Up to now we are not aware of any solvent that dissolves amphiphilic ligand diTegIPDoPy well. The strongly apolar tri-dodecyloxy diDoIPDoPy ligand is solubilized by aromatic solvents; this is in line with the extended aromatic core of the ligand, and in fact all ligands can be expected to dissolve in aromatic solvents.

The ligands' solubilities are likely to be reflected in their proton spectra: As can be seen in Figure 16, the apolar diMIPPy and 2,6-di(imino-4-dodeoxyphenyl)pyridine (diDoIPPy) produced coupling-resolved spectra in $CDCl_3$, while the amphiphilic diTegIPDoPy gave broader signals in which only the coupling of phenylic protons was observed. Amphiphilic structures often generate broad peaks in magnetic resonance studies, as they tend to form assemblies on the meso-scale that prevent rotational averaging of the magnetic fields around the molecules. A ^{1}H-NMR spectrum of a DMSO-d_6 solution of this ligand showed even broader peaks and was unsuitable for analysis. Therefore, both polar and apolar solvents seem to induce aggregation of the amphiphilic ligand. As clear solutions could be obtained in both $CDCl_3$ and as DMSO-d_6, the aggregation leads to structures of a finite size.

Thus, it was shown that the aniline and pyridinedicarbaldehyde building blocks react to form diverse diiminophenylpyridine ligands in good purity and acceptable yields. It was not always possible to find a practical solvent for these compounds, but all of them could be handled as dispersions in acetonitrile. The next two Sections document their association with platinum(II) and palladium(II) ions from a dichloro-salt, starting from the diMIPPy model ligand and continuing with functionalized ligands (Section 2.2.3).

2.2.2. Platination and palladination of the 2,6-di(4-methoxyiminophenyl)pyridine model ligand

The 2,6-diiminophenylpyridine pincer motive has previously been shown to coordinate to ions of, amongst others, copper,[35] ruthenium,[36] cobalt,[37] iron,[37] rhodium,[38] and nickel.[37] However, its potential to coordinate palladium and platinum appears to be less explored. While the insertion of a platinum ion into a N^N^N diimine ligand is only reported for platinum in the (IV)-oxidation state,[39] there are several examples of a palladium complexes with diiminophenylpyridine ligands.[21,40–43] Therefore, the model

complex of diMIPPy with Pd(II) was chosen as the starting point for further investigation on pincer-metal complexation, which was then extended towards complex formation with Pt(II) ions.

2.2.2.1. Coordination strategies for Pt(II)/Pd(II) to diMIPPy

Coordination reactions of transition metal ions with tridentate nitrogen ligands typically employ chloride salts of the metal ions.[40,44] An exchange of the chloride ligand with a more labile ligand would then involve a cation that binds chloride more strongly than the metal. Silver salts are commonly used for this purpose, and the exchanged silver chloride has to be removed after ion metathesis. However, silver ions themselves are known to form complexes with both π-donors[45] and N-donors,[46,47] which are both characteristics of our ligands. Initially, to avoid contamination of our products with Ag-ligand complexes, we opted for a chloride-free starting point in our synthesis of palladium-pincer complexes, as shown in Figure 17. The chlorine-free $Pd(NCCH_3)_4(BF_4)_2$ salt was available from commercial sources. Inconveniently, the corresponding Pt(II)-salt was not. Therefore, the chlorine-containing $Pt(II)(NCCH_3)_2Cl_2$ was used for the synthesis of platinum complexes.

These two coordination strategies were assessed with the diMIPPy model pincer, as shown in Figure 17. In these reactions, the solid diimine is weighed and transferred into a reaction flask, followed by addition of the other solid reactants as solutions in acetonitrile. An obvious difference in these approaches is the use of silvertetrafluoroborate in the platination (**(b)**, Figure 17) in order to displace the chloride counter-ion. This results in precipitation of silver chloride from the reaction solution, which is easily removed by filtration over Celite. Remarkably, the yellow diMIPPy solution turned deep red a few seconds after addition of a solution of the palladium(II) ditetrafluoroborate salt, while solutions of diMIPPy and the dichloroplatinum salt were always yellow. Both complexes were purified by precipitation from solutions of the (filtrated) crude in a minimal volume of acetonitrile with a large volume (around 200 mL) of diethyl ether.

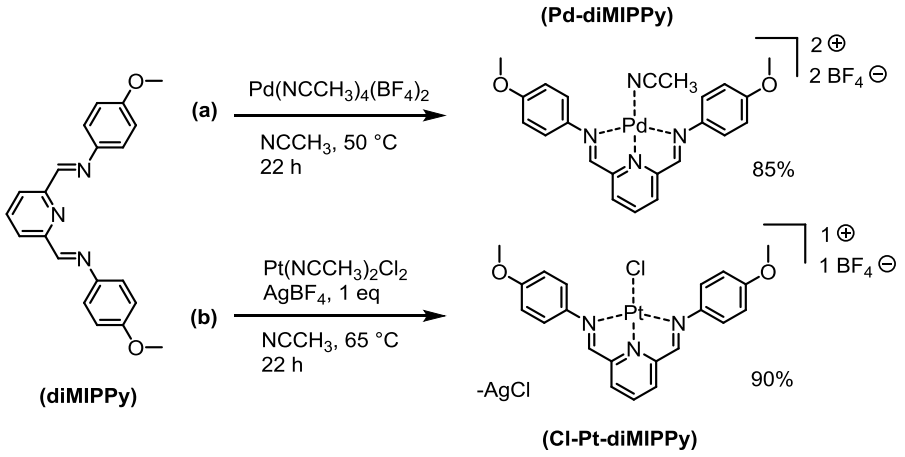

Figure 17: Coordination of diMIPPy to **(a)** a palladium(II) ion from the chloride-free tetrakis(acetonitrile)-di(tetrafluoroborate) salt, and **(b)**, to a platinum(II) ion from the chloride-containing *cis*-bis-(acetonitrile)-dichloride salt.

Figure 18 shows ^{1}H-NMR spectra collected for the two precipitated metal complexes Pd-diMIPPy and Pt-diMIPPy, and for free diMIPPy as a reference. While free diMIPPy is sparsely soluble in acetonitrile at room temperature, the solubility of its metal complex is at least 0.5 mg mL^{-1}, giving deep red and yellow solutions for respectively the Pd and Cl-Pt complexes. NMR spectra show another striking feature of these metal complexes: upon metalation of the ligand, the protons at the *para*- and *meta*- positions (protons **a** and **b** in Figure 18) of the central pyridine ring are exchanged for both complexes. These coordination-induced shifts are in complete agreement with what was reported previously for Pd-diMIPPy.[21]

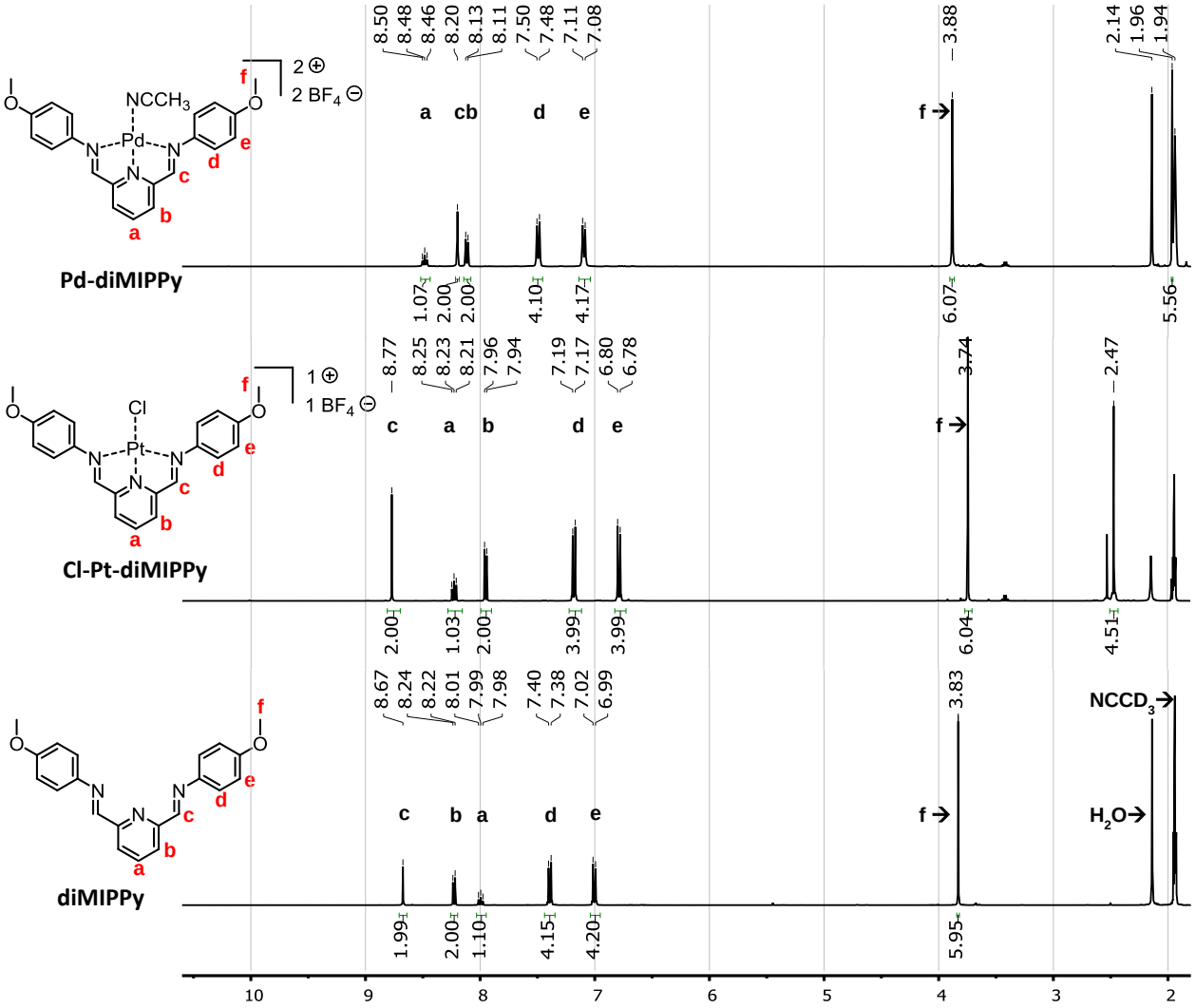

Figure 18: ^{1}H-NMR (400 MHz, CD_3CN) spectra of the palladium(II)-coordinated, chloroplatinum(II)-coordinated and free model ligand diMIPPy. The x-scale (chemical shift in ppm) has been adjusted to show the absence of an aldehyde peak around 10 ppm.

Interestingly, the imine protons of the Pd-bound diMIPPy shift upfield with respect to the free ligand, while they shift downfield when the ligand is bound to Pt. The anisyl protons show the opposite behaviour, and as a result the total width of the aromatic region shrinks for the Pd complex, while it

expands for the Pt structure. For Cl-Pt-diMIPPy, additional evidence for the successful formation of metal-ligand complexes comes from low resolution ESI-MS: an intense peak appears around 575 Da, which is the mass of the counter-ion free cationic complex (Figure 19). Finally, even though the imine starting materials (also see Figure 16) generally contain up to 5% of aldehyde, no aldehyde peaks are found in the present NMR spectra. Even more, solutions of the Cl-Pt-diMIPPy were found to be quite stable for at least two weeks in a non-anhydrous acetonitrile solution, with only traces of the free aldehyde forming over time. Thus, the metal ion acts as a template for imine formation, even in the absence of a dessicant.[21]

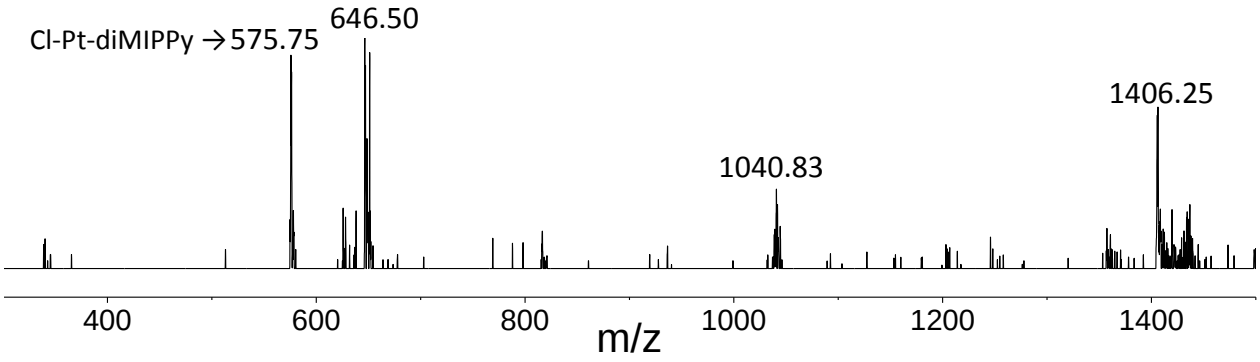

Figure 19: Low-resolution ESI-MS spectrum of Cl-Pt-diMIPPy. The origin of peaks other than 575.75 are unknown.

For Pd-diMIPPy, we did not observe the labile acetonitrile ligand that is suggested (without evidence) to occupy the forth coordination site at the metal ion.[21] Its three methyl protons are expected to resonate at a frequency distinct from the CD_3- (1.94 ppm) and CH_3- (1.96 ppm) signals from respectively deuterated and non-deuterated acetonitrile solvents residuals. This is not seen: there is no signal between water (2.1 ppm) and the methoxy protons (3.9 ppm). Thus, the acetonitrile ligand is either *not* coordinated to the Pd ion when Pd-diMIPPy is dissolved, or it is exchanged faster than the NMR timescale.

2.2.2.2. Acetonitrile ligands in Cl-Pt-diMIPPy

Contrarily, Cl-Pt-diMIPPy *does* show two intense resonances around 2.5 ppm, as shown and discussed in detail in Figure 20. In ^{1}H-^{13}C heteronuclear NMR experiments (HMBC, HSQC), these were found to couple to two carbon resonances not more than 5 ppm away from the acetonitrile carbons. Additionally, these peaks had an unusual lineshape with a sharper peak and a broader tail than a gaussian. We conclude that these resonances correspond to Pt(II)-coordinated acetonitrile.

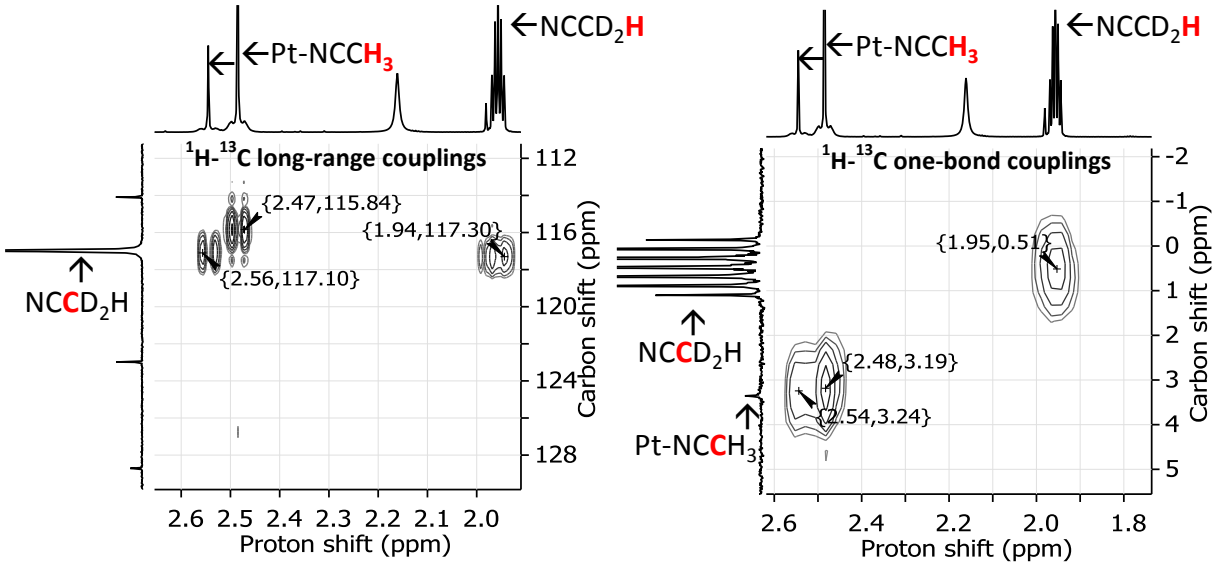

Figure 20: HMBC (left) and HSQC (right) ^{1}H-^{13}C heteronuclear correlation spectra of Cl-Pt-diMIPPy in CD_3CN. In the HMBC spectrum, two crosspeaks appear very close to the ^{13}C resonance of the CD_3CN cyanide carbon. These correspond to unusually shaped proton peaks that possibly correspond to Pt-coordinated acetonitrile. In the HSQC spectrum, these peaks cross with a ^{13}C resonance very close to that of the carbon of deuterated acetonitrile, suggesting that the molecule is indeed very similar to acetonitrile.

This implies that either **1)** the chlorine atom in Cl-Pt-diMIPPy is not a ligand but a counter-ion and acetonitrile can therefore bind to the forth coordination site, or **2)** that the isolated solid contains multiple Pt(II)-acetonitrile species. Since two peaks are observed that can be attributed to Pt-coordinated acetonitrile, **1)** and **2)** can both be true at the same time. Figure 21 shows possible structures that would give signals in NMR due to platinum-coordinated acetonitrile.

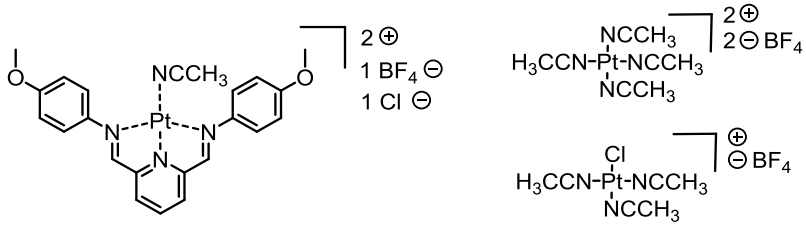

Figure 21: Possible origins of the resonances putatively assigned to Pt-coordinated acetonitrile in Figure 20.

Presence of these structures means that some of the platinum salt would not end up in pincer complexes. As in addition to this, the pincer ligand is highly unstable in free form, this would imply presence of either the free ligand and its aldehyde and aniline constituents, which are not present in the purified solid, not even in trace amounts. Moreover, the structures drawn in Figure 21 were not found in the mass spectrum, which showed only an intense peak corresponding to an $[M+1]^+$-particle (Figure 19). Consequently, the origin of the resonances at 2.5 ppm is unknown. It would be interesting to perform the

reaction in a non-coordinating solvent (MeOH) in the presence of a known amount of acetonitrile, to find out whether it indeed competes with the ligand for positions in the platinum(II) ligand field. Alternatively, ^{195}Pt-NMR could show the amount of distinct Pt-bonded species in solution.

In an analogous procedure to obtain a Pt-bound diMIPPy complex, the reagents were heated in DMSO instead of acetonitrile. After filtration of the intensely red suspension and precipitation with diethyl ether, a red solid was obtained that showed a similar exchange of the chemical shifts of the *para*- and *meta*- protons in the pyridine ring. However, the imine protons integrated to one instead of two, when compared to the integral of the central pyridine proton. No masses corresponding to the complex were found in the ESI mass spectrum, and we concluded that DMSO is not a suitable solvent for the reaction. Nonetheless, NMR showed that the species formed in DMSO solution was at least 80% pure, and that no aldehyde was present. The identity of the DMSO-borne structure is an ongoing question, and DMSO has been excluded from any operation on metal-di(iminophenyl)pyridine complexes to prevent competition between this solvent and the tridentate ligand.

In short, the di(iminophenyl)pyridine motive can be coordinated to platinum(II) and palladium(II) ions upon heating in acetonitrile solution, with the possibility to exchange chlorine counter-ions by using a suitable silver salt. The platinum(II) motive was chosen for investigation on functionalized ligand-metal complexes, because previously reported tridentate-platinum(II) complexes displayed interesting self-assembly properties and luminescence upon aggregation.[16–18,48] In the next Section, results from synthesis of functionalized pincer-platinum(II) complexes are presented.

2.2.3. Synthesis of Pt(II) complexes of functionalized 2,6-diiminophenylpyridine ligands

In this work, two attempts at platination of functionalized di(iminophenyl)pyridine ligands are described. Discussed is the platination of amphiphilic ligand diTegIPDoPy and hydrophilic diTegIPPy with methods highly similar to those used for the model ligand.

2.2.3.1. Synthesis of an amphiphilic platinum(II) complex

Figure 22 illustrates platination of amphiphilic ligand diTegIPDoPy. In contrast to the model reaction, the platinum salt was added in a slight excess. The crude, evaporated reaction mixture was a pale yellow powder that resisted dissolution in polar, apolar and aromatic solvents ($CHCl_3$, MeOH, $NCCH_3$, $CHCl_3$:MeOH (1:1), $CHCl_3$:$NCCH_3$ (1:1), 1,4-dioxane, 1,2-dimethoxyethane, EtOH and *n*-BuOH). Nonetheless, an ^{1}H-NMR of a dispersion of the crude in CD_3CN gave some evidence of a complete conversion of the imine starting material. Figure 23 shows ^{1}H-NMR spectra of CD_3CN dispersions of both the crude complex as well as the ligand.

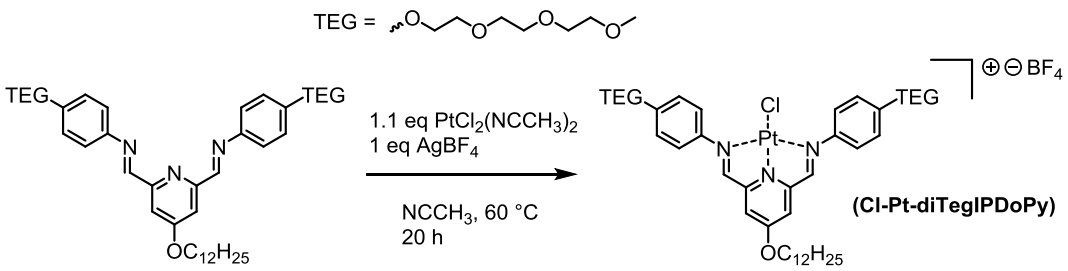

Figure 22: Platination of amphiphilic ligand diTegIPDoPy with *cis*-bis(acetonitrile)-dichloroplatinum as a platinum(II) donor and silvertetrafluoroborate to exchange the counterion.

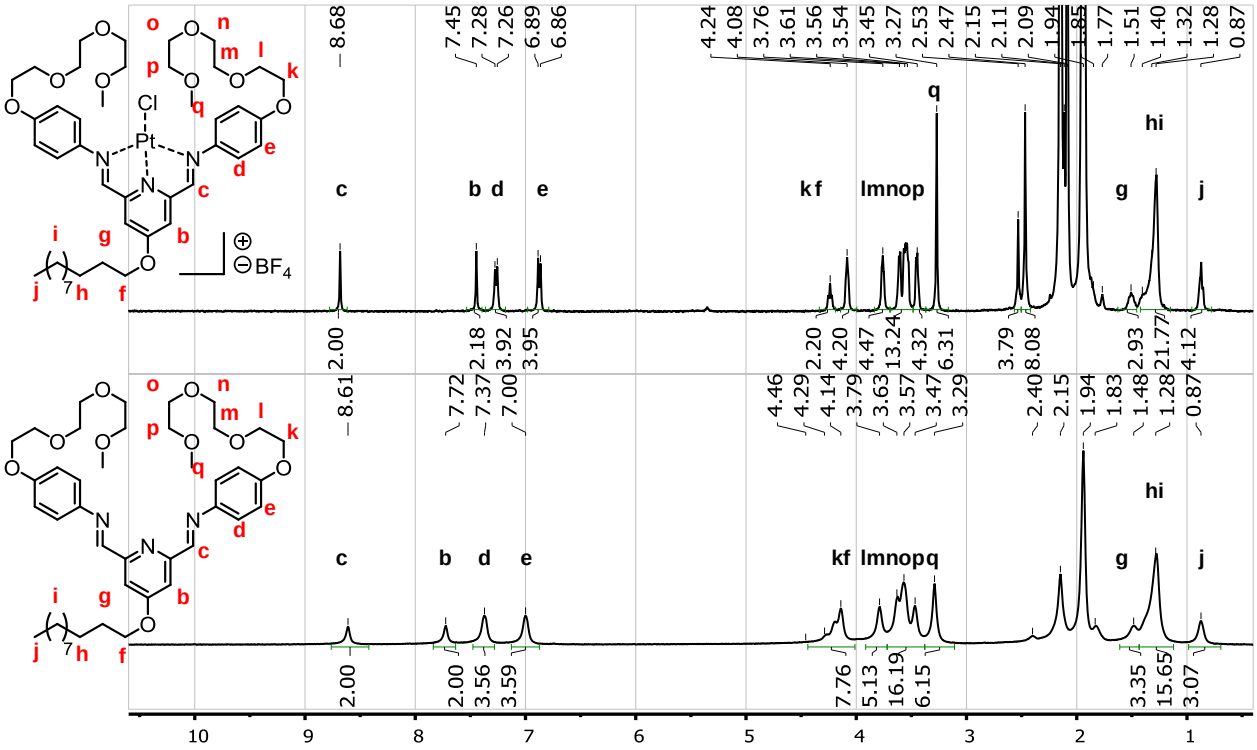

Figure 23: ^{1}H-NMR (400 MHz, CD_3CN) of (top) chloroplatinum complex Cl-Pt-diTegIPDoPy and (bottom) the free ligand diTegIPDoPy.

A comparison of the spectrum of the ligand in CD_3CN dispersion and $CDCl_3$ solution (Figure 16, bottom) reveals a remarkable broadening of the resonances in the former. Likely, this reflects diTegIPDoPy's insolubility in acetonitrile. Nonetheless, the former spectrum is useful to compare the chemical shifts of the resonances in the pyridine ring. This comparison reveals a much less obvious rearrangement of peaks than observed upon complexation of the model ligand to Pt(II) (see the two lowermost spectra in Figure 18). The *meta*-resonance (proton **b** in Figure 23) in diTegIPDoPy shifts 0.17 ppm upfield, which is less than the difference of 0.28 ppm found for the model Pt-ligand complex. Additionally, the amphiphilic ligand lacks the *para*-proton in its pyridine ring, which was a very clear probe for complex formation in the model ligand. At δ=2.11 ppm and 2.15 ppm, new resonances appear in the spectrum of the complex. These were also observed for the model ligand and discussed in great detail (Figure 20).

Nonetheless, all resonances of the complexed ligand shift according to the trends established for the model ligand, and the spectrum shows a complete absence of aldehyde. This supports our tentative conclusion that the main constituent in the crude is Cl-Pt-diTegIPDoPy. The relative sharpness of the peaks also suggests that acetonitrile might be a good solvent for the isolated complex. A small sample of the crude powder was dissolved in acetonitrile and filtrated over Celite to remove AgCl. The filtrate was concentrated to a yellow oil that was indeed soluble in acetonitrile. However, NMR showed dialdehyde and monoaldehyde peaks that contribute to at least 30%, while the crude showed a complete absence of aldehyde peaks.

A possible explanation for the instability of the complex in acetonitrile is the relative insolubility of the ligand with respect to the platinum complex, which dissolves readily in acetonitrile. As a result, the free ligand can escape equilibrium upon dissociation of the complex, and the imines of the free ligand can quickly hydrolyse. Therefore, if the timescale of Pt(II)-ligand dissociation is short enough, precipitation will drive the hydrolysis of the imine bonds, even though the Pt(II)-tridendate ligand would be more stable.

2.2.3.2. Synthesis of a di-tri(ethylene glycol)-bearing diiminophenylpyridine-Pt(II) complex

Since the reaction conditions and purification strategy that gave a pure Pt-ligand complex for the model ligand were found to be less applicable to a ligand with amphiphilic derivatization, we attempted platination of the di-TEGylated hydrophilic ligand diTegIPPy. This latter ligand is more soluble in acetonitrile, and has the *para*-proton on the pyridine ring that has shown to be a useful probe for Pt binding (Figure 22). As illustrated in Figure 24, we used two instead of one equivalent of silver tetrafluoroborate for Pt^{2+}-insertion into diTegIPPy. This was done to allow access to the full square-planar complexes with monovalent ligands (Section 2.3) without the need for another filtration to remove the silver chloride by-product.

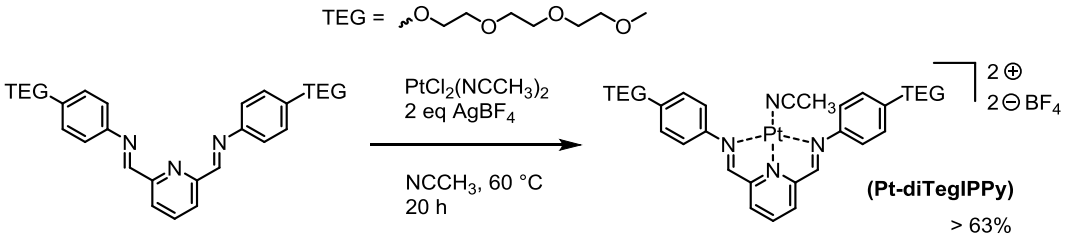

Figure 24: Synthesis of hydrophilic platinum(II)-ligand complex Pt-diTegIPPy**.**

Silver chloride was removed from the crude by filtration over Celite and the filtrate was concentrated under reduced pressure. This resulted in a wax with, again, a much improved solubility with respect to the free ligand. It gave clear, orange solutions in CD_3CN and $CDCl_3$, of which the former solution gave well-resolved NMR signals. The spectrum is shown in Figure 25. Similarly to what was observed for the model ligand, the central pyridine proton and its neighbour exchange upon complexation to Pt^{2+} (protons **a** and **b**). However, the spectrum gave evidence of mono-imine, aldehyde and aniline impurities in similar concentrations as found for amphiphilic complex Cl-Pt-diTegIPDoPy.

Thus, either the formation of the complex was not complete after 20h, or work-up resulted in partial hydrolysis of Pt-diTegIPPy. Further purification was attempted by another filtration over Celite and precipitation from a minimal volume of acetonitrile with diethyl ether. While this did not result in any further hydrolysis, the purity of the complex did not improve.

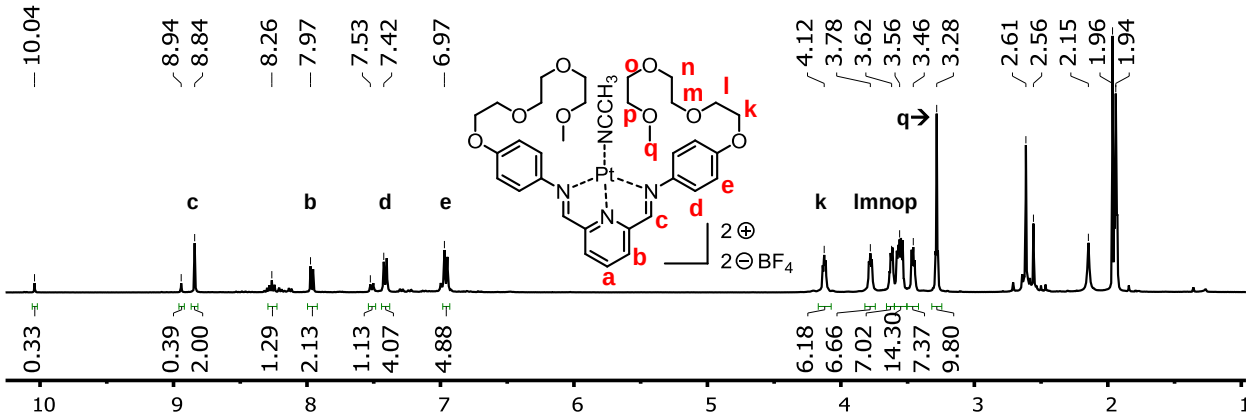

Figure 25: ^{1}H-NMR (400 MHz, CD_3CN) of hydrophilic complex Pt-diTegIPPy with mono-imine and aniline impurities.

2.2.3.3. On the relevance of ligand and complex solubilities for Pt^{2+}-insertion into diimino-phenylpyridine ligands

Judged by the absence of further hydrolysis upon additional purification of the hydrophilic Pt-diTegIPPy complex, it is reasonable to conclude that the complex did not fully form in the first place, that the resulting uncoordinated ligand hydrolyzed during work-up, and that, therefore, the present work-up strategy does not satisfactorily remove the hydrolyzed by-products. This suggests that the reasons for the impurities found in the amphiphilic complex Cl-Pt-diTegIPDoPy and the hydrophilic complex Pt-diTegIPPy are subtly different: the former the complex was initially intact and only hydrolyzed upon purification, while the latter did not seem to be formed completely.

Possibly, the slight excess of Pt(II) salt in the diTegIPDoPy Pt-insertion supressed competition of acetonitrile with the nearly insoluble free ligand. For hydrophilic diTegIPPy, no excess was used and the reaction was not complete to begin with. Again, as the product is more soluble than the ligand, competition reactions with the solvent and reformation of the starting material are *not* supressed.

To diagnose the problems and improve synthesis of these complexes it is advised to reattempt them **1)** in non-coordinating solvents, **2)** with stoichiometric amounts of acetonitrile to assess the relevance of solvent competition, and ideally, **3)** in a solvent system that holds the ligand in solution but releases the complex to remove it from equilibrium. When necessary, the solubilities of the ligands and complexes can be compared by using corresponding ketimine ligands, in which the imine bond is *not* in dynamic equilibrium and therefore *not* hydrolyzed upon release from the complex. In our ligands, the solubilities seem to be mainly determined by the large substituting dodecyloxy and tri(ethylene glycol) chains, and therefore a change to ketimine complexes should not significantly change the solubilities.

2.3.Interaction of pincer-platinum complexes with monovalent ligands

In order to create stable, soluble, square planar Pt(II)/Pd(II)-ligand complexes that have a tendency to form aggregates of a controllable morphology, a ligand-metal system was developed that can be easily assembled from modules that give a polar or apolar character at a certain position in the complex. With the successful synthesis of the model complexes Pd-diMIPPy and Cl-Pt-diMIPPy, it is possible to occupy three out of four of the coordination sites of Pt(II) and Pd(II) ions. Here, the feasibility of coordination of 4-methoxyphenylisocyanide with Pt-diMIPPy is studied, and next the possiblity of synthesis tridendate-metal-ligand complexes with pyridines by using the model complex Pt-diMIPPy and hydrophilic complex Pt-diTegIPPy.

2.3.1. 4-Methoxyisocyanide forms an insoluble precipitate with Pt-diMIPPy

Figure 26 illustrates our attempt to coordinate 4-methoxyphenylisocyanide to Pt-diMIPPy. When 4-methylisocyanide and Pt-diMIPPy were mixed in MeOH, they gave rise to a faintly yellow solution. A sample was taken for NMR 5 minutes after mixing, and the rest of the reaction mixture was worked up after 20 h of stirring at room temperature. A white precipitate was removed by filtration over Celite on glass, and the filtrate was evaporated to dryness and redissolved in 1 mL of acetonitrile. Precipitation in diisopropyl ether gave a brown solid, which was also subjected to NMR analysis .

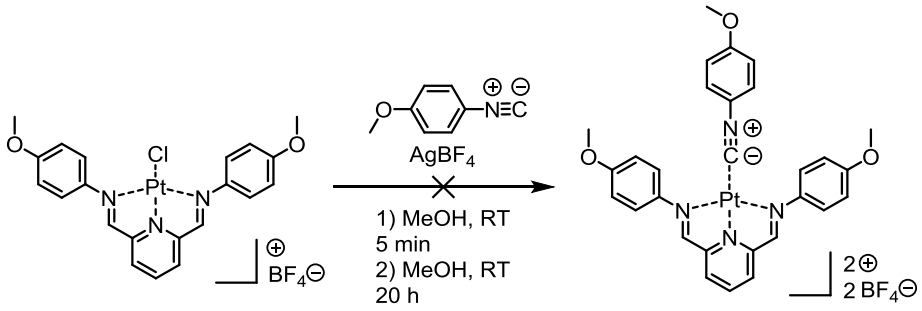

Figure 26: Attempt at coordination of 4-methoxyphenylisocyanide to the model Pt-diMIPPy complex.

Unfortunately, the identity of species in these samples is elusive, as they give very broad, unresolved features. Moreover, the precipitate is practically insoluble in acetonitrile, whereas both reagents are. ESI-MS showed no peaks that were identifiable as our ligand or any complex. While the reaction product cannot be identified, a possible explanation for these problems is the nucleophilicity of the isocyanide carbanion towards imines, as exploited in the Ugi reaction. It is worthwhile to explore more stable imines with isocyanides, such as ketimines rather than aldimines. Additionally, the experiment could be done on a small scale in deuterated solvent to rule out degradation during work-up.

2.3.2. Pt(II)-di-(imino-4-methoxyphenyl)pyridine complexes with pyridine and 4-picoline

Inspired by the sub-component self-assembly reaction of Nitschke and co-workers,[21] in which Pd^{2+} ions template pyridinedicarbaldehydes and anilines into pincer-metal complexes *in one step*, we chose a similar one-step, multicomponent approach as a starting point for the synthesis of two-ligand, square-planar Pt^{2+} complexes. This approach is illustrated in Figure 27.

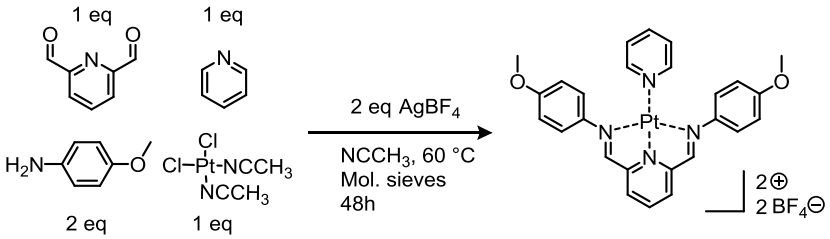

Figure 27: Attempt at a one-step synthesis of a square-planar Pt(II)-complex with a tridentate and monovalent ligand.

Within 16h, the mixture turned from a yellow solution to a dark green, turbid mixture. After 48h, it was filtrated to remove molecular sieves and silver chloride, and the green solution was concentrated to a small volume under reduced pressure. A green solid (29% by mass of the envisioned product) was precipitated with diethyl ether, and a spectrum of its CD_3CN solution is shown in Figure 28, accompanied with a spectrum of Cl-Pt-diMIPPy for comparison. Clearly, it indicates formation of a highly similar platinum complex to what was found for complexation of Pt(II) with the pre-formed diMIPPy ligand (Section 2.2.2). Additionally, there are some higher-order signals around 8.7 and 7.5 ppm that lie close to the expected shifts for pyridine that is free in a CD_3CN solution (7.3, 7.7 and 8.6 ppm). However, correlation spectroscopies (COSY, HSQC and HMBC) revealed no correlation between these peaks, and therefore they are possibly impurities, rather than complexed pyridine.

ESI-MS of a acetonitrile solution of the precipitated complex, given in Figure 29 showed peaks corresponding to $[M+H]^+$ of the free ligand (found: 346.1539 Da, calculated: 346.1556) and to $[M]^+$ of a silver-bound dimer of the ligand (found: 799.1977 Da, calculated: 799.1977). By similarity of the proton spectra of the product from subcomponents and the model reaction (Figure 18, middle spectrum), it seems unlikely that the Ag(I)-dimer is indeed the product observed in solution. However, these ESI-MS results show that there are Ag(I)-ions in reactions, and possibly Ag(I)-bound pincer complexes as well. It is of great interest to repeat this reaction using the silver-free Pd(II)-system, or with a chloride-free Pt(II)-salt.

Because it was unclear whether the new asymmetric peaks (Figure 28, inset) corresponded with pyridine that was complexed or free, or with an impurity such as Ag-bound pyridine, the putative pincer-platinum-pyridine complex was reacted with another pyridine. Therefore, added 2.0 equivalents of 4-picoline were added: Instead of broad, asymmetric peaks it gives two sharp doublets along with a sharp methyl peak at 2.34 ppm. A report by De Cola and co-workers claimed symmetric, well-resolved resonances from Pt(II)-coordinated 4-substituted pyridines in CD_2Cl_2.[17,18]

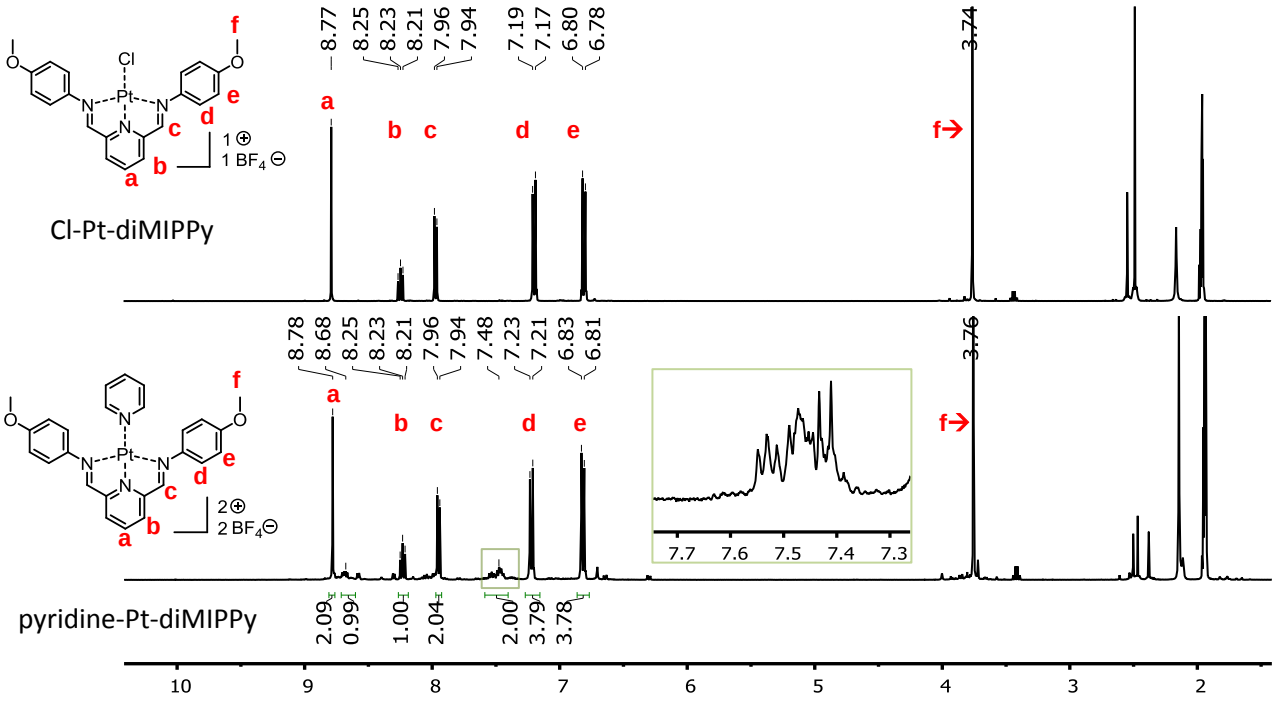

Figure 28: ^{1}H-NMR (400 MHz, CD_3CN) of (top) Cl-Pt-diMIPPy and (bottom) of isolated solid from a reaction of 4-methoxyaniline, 2,6-pyridinedicarbaldehyde and pyridine. Inset: magnified region of the region between 7.3 and 7.7 ppm that shows a highly asymmetric multiplet.

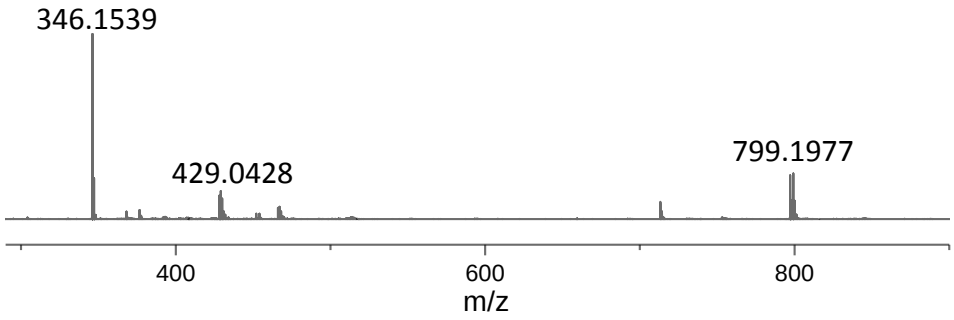

Figure 29: High-resolution ESI-MS of the precipitated solid from the pyridine-Pt(II)-diMIPPy multicomponent synthesis.

A proton spectrum was recorded just after mixing a CD_3CN solution of the purified material from the subcomponent reaction with 4-picoline at RT. As expected, 4-picoline appeared as two double doublets at 8.40 and 7.17 ppm in a 2:1 ratio with the complex previously synthesized. Thus, as all signal from two equivalents of 4-picoline was recovered in the peak expected for the free compound, there is no complex formation at room temperature. Next, the very same NMR sample was stirred for 20h at 60 °C. Another spectrum was recorded. This experiment is illustrated in Figure 30.

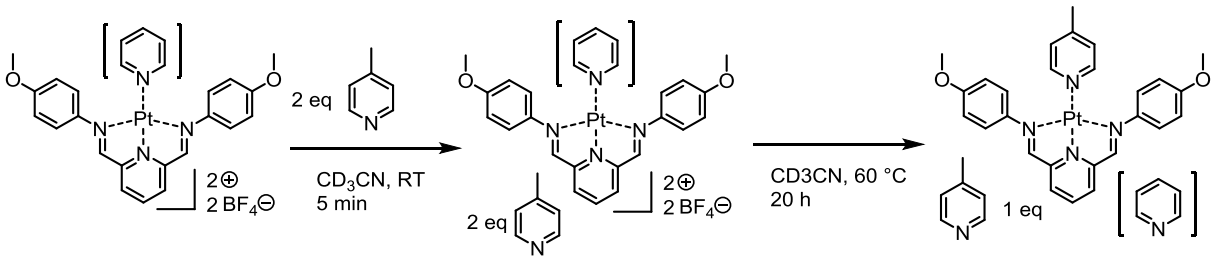

Figure 30: Coordination of 4-picoline with model complex Pt-diMIPPy, to find out whether indeed pyridine is bound (drawn in brackets). In the first step, complex an 4-picoline are mixed together at RT to determine the shifts of 4-picoline in the solvent. In the second step, the same mixture is heated (60 °C, 20 h) to generate the complex.

Figure 31 shows the spectrum after heating in black, superimposed on the spectrum taken directly after mixing in grey. The amount of aldehyde slightly increased to around 5% after heating, but was deemed insignificant. Thus, pyridines do not compete with metal-pincer binding even when mixed, present in small excesses, or heated for long periods. Again, new "scrambled", asymmetric aromatic resonances appear after heating with a new pyridine. Thus, the behaviour of both 4-picoline and pyridine after being heated with Pt-diMIPPy is similar.

While the imine proton and the anisyl protons appear similar to their positions before heating, the protons on the pyridyl base of the diMIPPY ligand (a,b) appear to be superimposed. In addition to this, the aromatic signals corresponding to 4-picoline in CD_3CN solution (8.40 and 7.17 ppm) only correspond to one equivalent after heating (as opposed to two before heating). We note the integral of the methyl signal of 4-picoline (2.34 ppm) reduces accordingly, with a new peak appearing slightly downfield. Thus, this suggests that one equivalent of 4-picoline could be coordinated to the pincer-platinum complex. The lost area under the peaks expected for 4-picoline in solution should then be recovered in the form of new peaks that corresponding to coordinated 4-picoline.

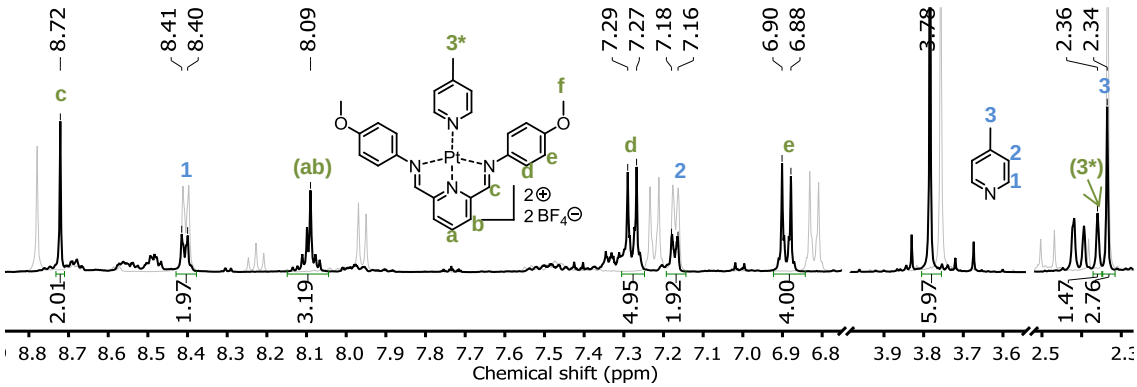

Figure 31: ^{1}H-NMR (400 MHz, CD_3CN, 293 K) of (black) a heated mixture (20h, 60 °C) of 4-picoline in solution and a possible pincer-platinum-pyridine complex, superimposed on (grey) a spectrum of the same mixture before heating (0h, RT). Peaks labeled in brackets are assigned putatively and need to be confirmed with appropriate correlation spectroscopy techniques before they can be assigned definitely.

Disappointingly, newly appearing aromatic peaks are again low in intensity and highly asymmetric, and we were not successful in recovering from them the integrated signal that would correspond to one equivalent of coordinated 4-picoline. The potential new peak that appears slightly downfield of the methyl signal from solution is surrounded by peaks that stem from impurities or Pt(II)-coordinated acetonitrile, and therefore we cannot assign it definitely without the help of correlation spectroscopy.

Thus, we conclude that our previously reported Pt-diMIPPy complex is also achievable from a subcomponent technique. However, it is unclear whether pyridine added as a subcomponent acts as a monovalent ligand. We found that mixing an excess of pyridine ligand with a platinum-pincer complex to which a pyridine is possibly coordinated *does definitely not* result in any coordination after mixing at room temperature, but possibly results in coordination when heated. If the latter is true, it results in "scrambled", asymmetric resonances for the coordinated pyridine. This could be confirmed in the future with correlation spectroscopies, and with mass spectrometry.

2.3.3. Pyridine-Pt-pincer complexes with tri(ethylene glycol) derivatizion on either the pyridine or pincer

Analogously to pyridine coordination to Pt-diMIPPy, coordination of 4-TEG-pyridine to Cl-Pt-diMIPPy in the presence of $AgBF_4$ was attempted, as well as coordination to the hydrophilic Pt-diTegIPPy. As illustrated in Figure 32, a yellow solution of $AgBF_4$ and Cl-Pt-diMIPPy was mixed with a colorless solution of 4-TEG-pyridine, the color changed to green in an instant. ^{1}H-NMR spectroscopy on a sample of the resulting solution in $CDCl_3$ revealed that the diMIPPy ligand was no longer bound to platinum, as the shifts matched exactly with the shifts of the free ligand. Moreover, the ratio of aldehyde to imine peak areas was 1-to-2, revealing that hydrolysis towards aniline/aldehyde was no longer suppressed. After 20 h without presence of a desiccant, measurement on the same sample was repeated. The ratios remained constant, and we conclude that they represent equilibrium between imine and aldehyde/aniline species in the presence of one equivalent of pyridine.

Heating (3 d, 40 °C) in the presence of molecular sieves resulted in the formation of precipitate. A sample was taken for NMR, and still showed a large amount of hydrolyzed species. Following removal of silver chloride by filtration, a wax was recovered evaporation of solvents. ^{1}H-NMR showed only broad peaks with unresolved coupling.

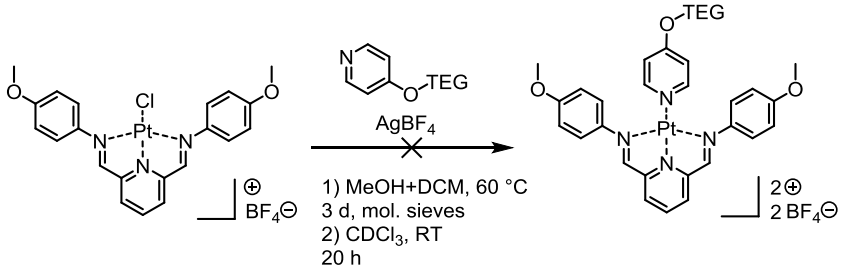

Figure 32: Attempt at coordination of 4-TEG-pyridine to complex Cl-Pt-diMIPPy.

ESI-MS on solid showed the free 4-TEG-pyridine as a $[M+H]^+$ ion (expected: 242.1387, found: 242.1379), diMIPPy as $[M+H]^+$ (expected: 346.1550, found: 346.1541) and a Ag(I)-bound diMIPPy dimer (expected: 797.2000, found: 797.1978). Therefore, it is reasonable to assume that this pyridine does not form a stable pyridine-platinum-pincer complex under these conditions, as the ligand is liberated from the metal within seconds, followed by its hydrolysis. Heating in presence of molecular sieves reforms neither the ligand, nor the complex.

In a similar attempt illustrated in Figure 33, hydrophilic complex Pt-diTegIPPy was stirred in methanol (3h, 40 °C) with 4-TEG-pyridine. Even though no silver salts were added, a precipitate formed. It was removed by filtration over Celite on glass to yield a black (very dark green) solution that was clear nonetheless. Precipitation with diethyl ether gave a sticky tar at -18 °C, which was washed by sonication with more ether. An ^{1}H-NMR measurement on its $CDCl_3$ solution showed only broad, asymmetric and unresolved peaks, with absence of aldehyde. The formation of precipitate points to the formation of insoluble byproducts with unknown identity. ESI-MS again shows the free 4-TEG-pyridine, along with the free pincer (expected: 610.3123, found: 610.3106).

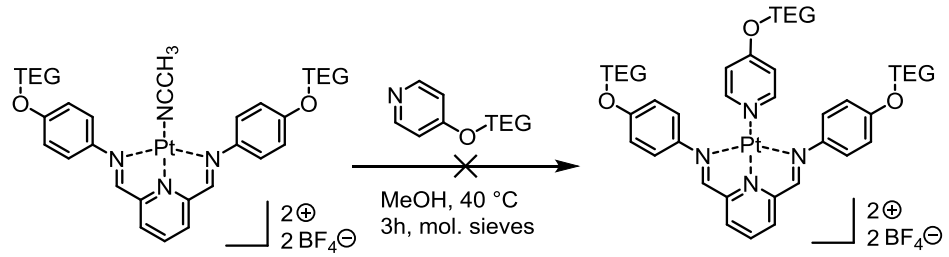

Figure 33: Attempt at coordination of 4-TEG-pyridine to complex Pt-diTegIPPy.

We conclude that the conditions attempted here do not give rise to coordination of 4-TEG-pyridine to platinum-pincer complexes. In the case of Pt-diMIPPy, the pyridine seemed to compete with the pincer for position in the Pt(II) ligand field, while for Pt-diTegIPPy, the proton spectrum shows no elements attributable to either ligands. In the former, the presence of Ag(I) possibly interferes with our envisioned reaction, and pyridine coordination to the corresponding Pd(II)-complex must be attempted, as those can be easily made without the need for silver ions.

3. Conclusion

In short, a metal-ligand motive was designed based on the previously known ligand 2,6-diiminophenylpyridine that is known to coordinate Pd(II) and other metal ions. The eventual goal of this project is to investigate the potential of these pincer complexes of Pt(II) and Pd(II) to aggregate into self-assembled structures, of which the morphology could be controlled by adjustment of solvent-ligand interactions by changing the character of substituents on the ligand.

By exploiting the ligand's modular synthesis from two equivalents of aniline and one equivalent on 2,6-pyridinedicarboxaldehyde, the motive's applicability was extended to highly polar and apolar media. To this end, a library of hydrophobic and hydrophilic 2,6-pyridinedicarbaldehydes and anilines was synthesized. From a library of two pyridinedicarbaldehydes and three anilines, five 2,6-diiminophenylpyridine pincer ligands were synthesized with hydrophilic, hydrophobic and amphiphilic characters.

Ions of Pt(II) and Pd(II) were found to coordinate 2,6-diimino-4-methoxyphenylpyridine, which served as a model for more hydrophobic or hydrophilic ligands. Complexation could easily be followed by ^{1}H-NMR, which witnessed strong coordination-induced shifts of the protons in the ligand. However, complexes of Pt(II) with hydrophilic or amphiphilic pincer ligands were unstable to either synthesis or purification by identical methods as those used for the model ligand. The most likely explanation for these problems is the high solubility of the complex as opposed to the near-insolubility of the free ligand in solvents used for reaction and work-up. As a result, reactions starting from the complex are promoted, and as a result the equilibrium favors starting materials or by-products. Complexation will be compared in different solvents to establish the relevance of ligand and complex solubilities, and to extend the ability to form Pt(II)/Pd(II)-complexes beyond the model ligand.

To allow even more control over the interactions of these complexes with solvents and their copies, the ability of Pt(II)-pincer complexes to coordinate a second, monovalent ligand was assessed. The model complex Pt(II)-2,6-diimino-4-methoxyphenylpyridine could be assembled from its aniline, dicarbaldehyde and metal sub-components in the presence of pyridine, but our spectroscopies were not able to unambiguously detect the presence of pyridine in the complex. Attempts to coordinate 4-tri(ethylene glycol)-pyridine to the model complex and its more hydrophobic counterpart with two pendant tri(ethylene glycol) chains resulted in either release of the ligand and hydrolysis of the imine bonds, or formation of an unknown product. Similarly, an isocyanide was found to react with the model complex, resulting in an unidentified species. The instability of our complexes in the presence of monovalent ligands will be studied by comparing the behavior of analogous Pd(II) and ketimine complexes. The latter is a convenient model for our dynamic imine complexes, because it offers a greater stability with very similar coordination behavior and solubility.

4. Outlook

Next to the specific suggestions to overcome the problems summarized in the Conclusion (Section 3), this Outlook suggests four broader lines along which the research described in this Thesis can be continued. The first two of these possibly address the problems with metalation of derivatized ligands and coordination of ancillary ligands, while the last two are truly continuations. These four are 1) a switch to silver-free systems, 2) studies on ketimines as opposed to aldimines, 3) self-assembly of metal-pincer complexes and 4) library extension towards new characters and multimetal systems.

4.1. The Pd(II) and Pt(II) tetrakis(acetonitrile) salts offer silver-free metalations

The metalation procedure for the Pt(II)-pincer complexes in this work relied on a chloroplatinum salt with $AgBF_4$ to abstract the chloride anion. However, it is possible that silver(I) also binds to the pincer ligands to form insoluble species that contaminate the various complexes in this work. These could be responsible for the unexpected results on coordination of pyridines with pincer-metal complexes. Therefore, it is advisable to compare these results with those from a silver-free system. This can be either a Pd(II)-complex with Pd(II) donated by tetrakis(acetonitrile) palladium ditetrafluoroborate salt, or the Pt(II) analogue. The latter was previously synthesized in our laboratory by a literature method.[49] Specifically, pyridine coordination to Pd(II)-diMIPPy should be attempted, as well as the formation of derivatized Pd(II)-pincer complexes. Alternatively, these complexes should be made from the Pt(II) tetrakis(acetontirile) ditetrafluoroborate salt.

4.2. Ketimine pincers to probe ligand and complex solubilities without hydrolysis

Next to silver(I) crosstalk, the low solubility of the free ligands as opposed to the corresponding complexes is likely to cause problems in the preparation of derivatized Pt(II)-pincer complexes and coordination of pyridines to Pt(II)-complexes. Therefore, it is recommendable to study the solubility of these structures in a wide array of solvents. However, because aldehyde-derived imines hydrolyse in any solvent, it is recommendable to study solubilities on a system that is more stable. Imines that are formed from ketones (Figure 34 shows a representative example) are not prone to hydrolysis, and are therefore fit for this purpose. It must be kept in mind that these C=N-bonds are *not* dynamic, and therefore the ketimine system represents only a model for our intended multi-responsive aldimine complexes.

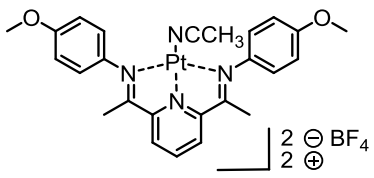

Figure 34: Ketimine equivalent of 2,6-di(imino-4-methoxyphenyl)pyridine-Pt complex.

4.3. Further projects: Self-assembly of metal-pincer structures and multimetal systems

When the derivatized 2,6-diiminophenylpyridine pincers successfully give metal complex complexes, the aggregates formed in water and organic solvents can be studied by a combination of light scattering, microscopy and rheological techniques next to “classical” organic chemistry methods such as NMR, UV/VIS and IR. A structure-activity relationship between introduced solvent-ligand interactions and aggregate morphology can then be deduced.

In addition to this, our building block library can be extended towards building blocks with other characters, such as perfluorinated, conjungated or ionic. Evenmore, building blocks for ligands with more than one metal-binding site more than one could be designed, in order to form oligo- or polymeric metal-ligand complexes. This will allow to construct a broad variety of multiresponsive organometallic materials by harnessing dynamic bonding and the imine-based modular design.

5. Acknowledgements

I am indebted to Maarten Smulders and Fátima García Melo for offering me the opportunity to do this research under their supervision. Because of your time and involvement, the period between November and April turned out to be pleasantly educational. Next to guiding me on a day-to-day basis and welcoming me for countless discussions on chemistry, you reviewed my manuscripts thoroughly on a very regular basis, resulting in this much improved account of my work of the last five months. Next, I am very grateful to Tom Wennekes for taking time to act as an additional examiner. Moreover, I express my gratitude to my laboratory colleagues at K180, Medea, Esther and Wang for helping me out and sharing many pleasant conversations. I thank Han Zuilhof for allowing me to work in his group for my third project at ORC. Finally, thanks to all people that work in this chair group for the warm atmosphere and friendly welcome.

6. Experimental section

6.1. Materials

4-Chloropyridine hydrochloride (99%), chelidamic acid hydrate (≥95%), 1-bromododecane (97%), sodium borohydride ($NaBH_4$,), oxalyl choride (≥99%), triethylamine (NEt_3, ≥99%), *N*-boc-aminophenol (97%), trifluoroacetic acid (TFA, 99%), 4-toluenesulfonyl chloride (≥99.0%), powdered potassium hydroxide (≥85%), sodium hydride (as a 60% dispersion in mineral oil), 1-dodecanol (≥98.0%), zinc oxide (ZnO, ≥99.0%), 4-methoxyaniline (≥99%), phosphorus(V) oxychloride ($POCl_3$, 99%), *cis*-bis(aceto-nitrile)dichloroplatinum(II) ($PtCl_2(NCCH_3)_2$), Tetrakis(acetonitrile)palladium(II) tetrafluoroborate ($Pd(NCCH_3)_4(BF_4)_2$), and Celite® 577 fine mesh (Celite) were obtained from Sigma-Aldrich (Germany) and used without further purification unless stated otherwise. Other materials were obtained from other commercial sources.

Chelidamic acid was stored in a desiccator and dried on a high vacuum pump for 24h prior to use. $NaBH_4$ was stored in a desiccator. When indicated, DMF and acetonitrile were distilled over phosphorus pentoxide and stored on molecular sieves. Similarly, when indicated, NEt_3 was distilled and stored over KOH pellets. When stated, glassware and K_2CO_3 were dried in an oven above 100 °C.

6.2.Methods

6.2.1. Synthesis of 4-hydroxypyridine, 2,6-diacetyl ester **(1)**

To a solution of dried chelidamic acid (5.37 g, 28.7 mmol) in 200 mL asbsolute EtOH was added 0.3 mL of H_2SO_4. The solution was stirred at reflux for 4 h. The mixture was concentrated under reduced pressure and dissolved in 500 mL of EtOAc. Crude **2** was extracted with 40 mL of saturated aqueous $NaHCO_3$. The aqueous layer was extracted five times with EtOAc until no product was found in it on TLC. The combined organic phases were dried over $MgSO_4$ and concentrated under reduced pressure to give **2** as a sticky solid in 61% yield (4.16 g, 17.4 mmol).

^{1}H-NMR (400 MHz, $CDCl_3$): δ 9.61 (s, 1H), 7.13 (s, 2H), 4.47 (q, J = 7.1 Hz, 4H), 1.42 (t, J = 7.1 Hz, 6H). R_f: 0.56 (SiO_2 in EtOAc, UV). Low-resolution MS (ESI): Expected 240.08 for $[M+H]^+$, found 240.17, expected 238.07 for $[M-H]^-$, found 238.00.

6.2.2. Synthesis of 4-dodecyloxypyridine, 2,6-diacetyl ester **(2)**

Under argon, a solution of **1** (4.16 g, 17.4 mmol) in a minimum volume of DMF, K_2CO_3 (5.77 g, 41.7 mmol) and one grain of 18-crown-6 were added to an oven-dried three-necked flask fitted with a reflux condenser, stop and Ar(g) inlet. After heating to 100 °C, 1-bromododecane (5.20 g, 20.9 mmol) was added with a syringe, and Ar(g)-flow was stopped. The suspensions was stirred for 20 h, concentrated under reduced pressure and resuspended in a mixture of EtOAc and ice water. The emulsion was poured into an extraction funnel, 50 mL of brine was added, and it was left standing for a week. The aqueous

layer was discarded and the organic and emulsified layer were combined, dried over $MgSO_4$ and concentrated under reduced pressure. The crude oil was purified with column chromatography on SiO_2 in DCM to yield **2** as a yellow oil in 36% yield (2.58, 6.33 mmol).

^{1}H-NMR (400 MHz, $CDCl_3$): δ (ppm) 7.77 (s, 2H), 4.47 (q, J = 7.1 Hz, 4H), 4.12 (t, J = 6.5 Hz, 2H), 1.83 (p, J = 6.7 Hz, 2H), 1.45 (t, J = 7.1 Hz, 6H), 1.27 (d, J = 6.7 Hz, 16H), 1.00 – 0.76 (t, 3H). ^{13}C-NMR (101 MHz, $CDCl_3$): δ (ppm) 167.17, 164.97, 150.27, 114.47, 69.18, 62.50, 32.05, 29.78, 29.76, 29.70, 29.65, 29.48, 29.40, 28.90, 25.99, 22.83, 14.35, 14.26. R_f: 0.15 (SiO_2 in $CDCl_3$:MeOH 24:1, UV). MS (ESI): Expected 408.2744 for $[M+H]^+$, found 408.2744.

6.2.3. Synthesis of 2,6-hydroxymethyl-4-dodecyloxypyridine **(3)**

To an oven-dried flask was added a solution of **2** (2.38 g, 6.05 mmol) in absolute EtOH (80 mL) and $NaBH_4$ (1.38 g, 36.6 mmol). The flask was fitted with a reflux condenser and stirred at 40 °C for 20 h, after which it was quenched with 100 mL of water. The mixture was concentrated under reduced pressure and the residue was redissolved in EtOAc and brine. The emulsion was transferred to a separation funnel and left standing for 24 h. The organic phase was removed, dried over $MgSO_4$ and concentrated under reduced pressure to give **3** as a white powder in 48% yield (1.54g, 4.77 mmol).

^{1}H-NMR (400 MHz, $CDCl_3$): δ (ppm) 6.69 (s, 2H), 4.68 (s, 4H), 4.00 (t, *J* = 6.5 Hz, 2H), 3.54 (s, 2H), 1.78 (p, *J* = 7.5 Hz, 2H), 1.55 – 1.39 (m, 2H), 1.33 (b, 16H), 0.88 (d, *J* = 7.0 Hz, 3H). ^{13}C-NMR (101 MHz, $CDCl_3$): δ (ppm) 166.59, 160.17, 105.55, 68.23, 64.42, 31.90, 29.64, 29.62, 29.56, 29.52, 29.33, 29.28, 28.85, 25.88, 22.68, 14.11. R_f: 0.33 (SiO_2 in DCM:MeOH 95:5).

6.2.4.Synthesis of 4-dodecyloxy-2,6-pyridinedicarbaldehyde **(4)**

An oven-dried three-necked flask was fitted with an Ar(g) inlet and two stops. Under Ar(g) flow, 30 mL of anhydrous DCM and 1 mL of oxalyl chloride was added, and the flask was cooled to -80 °C using a mixture of acetone/N_2(l). 2 mL of anhydrous DMSO in 10 mL of anhydrous DCM was added, and the mixture was stirred for 15 min. With a dropping funnel, a solution of **3** (1.54g, 4.77 mmol) in 200 mL of anhydrous DCM was added dropwise. After stirring for 1h, 7 mL of NEt_3 was added to the mixture, and it was allowed to reach RT. The solution was washed seven times with a 1:1 mixture of bleach and water, dried over $MgSO_4$, and concentrated under reduced pressure. The residue was redissolved in DCM, washed with water, dried over $MgSO_4$ and concentrated under reduced pressure. The residue was purified by column chromatography on SiO_2 with a gradient from heptane to heptane:EtOAc (6:1) to yield **4** as silvery crystals with an intense strawberry-like aroma in 52% yield (0.80 g, 2.50 mmol).

^{1}H-NMR (400 MHz, $CDCl_3$): δ (ppm) (s, 2H), 7.63 (s, 2H), 4.14 (t, *J* = 6.5 Hz, 2H), 1.84 (p, *J* = 7.5 Hz, 2H), 1.50 – 1.41 (m, 2H), 1.27 (b, 16H), 0.88 (d, *J* = 7.0 Hz, 3H). ^{13}C-NMR (101 MHz, $CDCl_3$): δ (ppm) 192.59, 167.28, 154.86, 111.63, 69.49, 32.05, 29.78, 29.76, 29.69, 29.64, 29.48, 29.37, 28.82, 25.95, 22.83, 14.26. R_f: 0.69 (SiO_2 in p.e. 40-60:EtOAc 2:1).

6.2.5.Synthesis of 4-dodecyloxy-*N*-boc-aniline **(5)**

This procedure was adapted from Ito and co-workers.[50] To a solution of *N*-boc-4-aminophenol (1.0 g, 4.78 mmol) in distilled acetonitrile (50 mL) in an oven-dried flask was added K_2CO_3 (1.32 g, 9.56 mmol) and 1-bromododecane (3.57 g, 14.3 mmol) and the mixture was stirred at reflux for 20 h. The suspension was concentrated under reduced pressure and the residue was redissolved in water/ether. The aqueous phase was extracted three times with ether, and the combined organic phases were dried with Na_2SO_4 and concentrated under reduced pressure. The residue was adsorbed to SiO_2 and purified on by column chromatography on SiO_2 in a gradient from heptane to heptane:EtOAc (1:1) to yield **5** as a white solid in 80% yield (1.446 g, 3.83 mmol).

^{1}H-NMR (400 MHz, $CDCl_3$): δ (ppm) 6.82 (d, J = 8.9 Hz, 2H), 6.31 (s, 1H), 3.91 (t, J = 6.6 Hz, 2H), 1.75 (p, J = 7.4 Hz, 2H), 1.50 (s, 9H), 1.42 (p, J = 7.4, 2H), 1.28 (b, J = 16.9 Hz, 16H), 0.92 – 0.82 (t, J=7.4 Hz 3H). R_f: 0.59 (SiO_2 in heptane:EtOAc 4:1, UV). MS (ESI): Expected 322.2377 for $[M+H]^+$, found 322.2363.

6.2.6. Synthesis of 4-dodecyloxyaniline **(6)**

To a flask containing **5** (1.446 g, 3.83 mmol) was added 15 mL of DCM and 10 mL of TFA. The flask was fitted with a stop, and the brown solution was stirred for 2 h. It was concentrated under reduced pressure, left on air for 14 d and purified by column chromatography on SiO_2 in a gradient from DCM:MeOH (100:2) to DCM:MeOH (100:5). The solid was dissolved in MeOH:DCM 1:9 and washed with a 1M solution of aqueous NaOH to yield **6** as a free aniline in 52% yield (0.550 g, 1.98 mmol).

^{1}H-NMR (400 MHz, $CDCl_3$): δ (ppm) 6.73 (d, J = 8.8 Hz, 2H), 6.63 (d, J = 8.8 Hz, 2H), 3.88 (t, J = 6.6 Hz, 2H), 3.30 (s, 2H), 1.72 (s, 2H), 1.45 (b, 2H), 1.27 (b, 16H), 0.89 (t, J = 6.6 Hz, 3H). R_f: 0.69 (SiO_2, in MeOH:DCM 5:95). MS (ESI): Expected 278.2478 for $[M+H]^+$, found 278.2486.

6.2.7.Synthesis of 4-toluenesulfonyl-methoxytri(ethylene glycol) **(7)**

This procedure from adapted from De Cola and co-workers.[17] To a solution of toluenesulfonyl chloride (3.66 g, 19.18 mmol) in anhydrous DCM (70 mL) in an oven-dried round-bottomed flask was added powdered KOH (2.05 g, 36.54 mmol). It was stirred for 5 hours at 0 C. Water was added, and the two-phase system was left for 3 d. The DCM phase was separated and washed with saturated aqueous $NaHCO_3$ and brine. The solution was dried over $MgSO_4$ and concentrated under reduced pressure to yield **7** (5.286 g, 16.60 mmol) as a colorless oil. Yield: 91%.

^{1}H-NMR (400 MHz, $CDCl_3$): δ (ppm) 7.80 (d, J = 8.2 Hz, 2H), 7.34 (d, J = 8.0 Hz, 2H), 4.16 (t, J = 5.0 Hz, 2H), 3.69 (t, J = 4.9 Hz, 2H), 3.65 – 3.56 (m, 6H), 3.56 – 3.50 (m, 2H), 3.37 (s, 3H), 2.45 (s, 3H). R_f: 0.39 (SiO_2, MeOH:DCM 2:98).

6.2.8. Synthesis of 4-methoxytri(ethylene glycol)-*N*-boc-aniline **(8)**

This procedure was adapted from Ito and co-workers.[50] To a solution of *N*-boc-4-aminophenol (1.60 g, 7.65 mmol) in acetonitrile in an oven-dried flask was added dried K_2CO_3 (2.97 g, 21.5 mmol) and **7** (2.28 g, 7.17 mmol). The flask was fitted with a reflux condenser and the mixture was refluxed for 24 h. The

suspension was concentrated under reduced pressure and the residue was redissolved in EtOAc and water. The organic layer was separated and washed twice with water, once with 1M aqueous NaOH, and again once with water. It was dried over $MgSO_4$ and concentrated under reduced pressure to yield **10** (1.829 g, 5.15 mmol) as an orange oil. Yield: 72%.

^{1}H-NMR (400 MHz, $CDCl_3$): δ (ppm) 7.24 (d, J = 9.1 Hz, 2H, overlaps with $CDCl_3$), 6.84 (d, J = 8.9 Hz, 2H), 6.33 (s, 1H), 4.10 (t, J = 5.4 Hz, 2H), 3.83 (t, J = 4.9 Hz, 2H), 3.76 – 3.70 (m, 2H), 3.70 – 3.62 (m, 4H), 3.57 – 3.51 (m, 2H), 3.38 (s, 3H), 1.50 (s, 9H). R_f: 0.40 (SiO_2 in MeOH:DCM 2:98).

6.2.9.Synthesis of 4-methoxytri(ethylene glycol)-aniline **(10)**

To a flask containing **8** (1.829 g, 5.15 mmol) was added 25 mL of DCM and 15 mL of TFA. It was stirred for 2h, and concentrated under reduced pressure. A DCM solution of the crude was washed with 1.2 M aqueous NaOH and was dried over $MgSO_4$ to give **10** (0.566 g, 2.22 mmol) as a brown oil. Yield: 43%.

^{1}H-NMR (400 MHz, $CDCl_3$): δ (ppm) 6.75 (d, J = 8.7 Hz, 2H), 6.63 (d, J = 8.6 Hz, 2H), 4.05 (t, J = 5.5 Hz, 2H), 3.81 (t, J = 5.2 Hz, 2H), 3.75 – 3.70 (m, 2H), 3.70 – 3.62 (m, 4H), 3.57 – 3.53 (m, 2H), 3.38 (s, 3H). ^{13}C-NMR (101 MHz, $CDCl_3$): δ (ppm) 151.95, 140.04, 116.37, 115.88, 77.33, 77.01, 76.69, 71.94, 70.76, 70.65, 70.56, 69.91, 68.14, 59.04. R_f: 0.54 (SiO_2 in MeOH:DCM 5:95).

6.2.10. Synthesis of 4-dodecyloxypyridine **(11)**

10 $^w/_w$ % aqueous NaOH was added dropwise to a solution of 4-chloropyridine (5.427 g, 36.2 mmol) in water until it turned pink. It was extracted three times with pentane, and the organic fractions were combined and concentrated under reduced pressure at RT to yield 2.0 mL (2.4 g, 21 mmol) of a yellow liquid. A dispersion of 60% NaH in mineral oil (1.27 g, 30.3 mmol) was deposited on a glass filter and washed with Et_2O. To an oven-dried flask under Ar(g) atmosphere was added 50 mL of distilled acetonitrile, and Ar(g) was bubbled through it for 30 min. Next, 1-dodecanol (4.7 g, 25.3 mmol), NaH and anhydrous DMSO (3 mL) were added. The mixture was stirred for 30 min at RT, and chloropyridine was added, and it was stirred for 3 d at 60 °C. The yellow solution was concentrated under reduced pressure and redissolved in EtOAc. The solution was washed twice with ice-water, dried over $MgSO_4$, and concentrated under reduced pressure. The residue was purified by chromatography on SiO_2 in a gradient from heptane:DCM (4:1) to DCM to DCM:MeOH (9:1) to yield **11** as a yellow solid in 16% yield (1.396 g, 5.90 mmol).

^{1}H-NMR (400 MHz, $CDCl_3$): δ (ppm) 8.47 – 8.32 (m, 2H), 6.82 – 6.73 (m, 2H), 3.99 (t, J = 6.5 Hz, 2H), 1.78 (p, J = 8.1 Hz, 2H), 1.51 – 1.38 (m, 2H), 1.26 (s, 16H), 0.88 (t, J = 7.7 Hz, 2H). ^{13}C-NMR (101 MHz, $CDCl_3$): δ (ppm) 165.04, 151.03, 110.24, 67.87, 31.90, 29.63, 29.61, 29.56, 29.52, 29.33, 29.30, 28.87, 25.91, 22.68, 14.11. R_f: 0.35 (SiO_2 in MeOH:DCM 5:95). MS (ESI): Expected 264.2322 for $[M+H]^+$, found 264.2321.

6.2.11.Synthesis of *N*-formyl-4-methoxyaniline **(12)**

This procedure was adapted from Hosseini-Sarvari and co-workers.[29] To powdered ZnO (0.331 g, 4.06 mmol) in a round-bottomed flask was added formic acid (0.92 mL, 25 mmol) and 4-methoxyaniline (1.00 g, 8.12 mmol). This was stirred for 2h at 70 °C. The mixture was dissolved in DCM and washed twice with water and once with saturated aqueous $NaHCO_3$, washed with $MgSO_4$ and concentrated under reduced pressure to yield **12** as a powder in 58 % yield (0.712 g, 4.710 mmol).

^{1}H-NMR (400 MHz, $CDCl_3$): δ (ppm) 8.50 (d, J = 11.5 Hz, 0.5H), 8.34 (d, J = 1.6 Hz, 0.5H), 7.45 (d, J = 8.9 Hz, 1H), 7.03 (d, J = 8.8 Hz, 1H), 6.93 – 6.83 (m, 2H), 3.81 (s, 1.5H), 3.80 (s, 1.5H). Purity (GC): 99%. R_f: 0.25 (MeOH:DCM 2:98). MS (ESI): Expected 152.0706 for $[M+H]^+$, found 152.0706.

6.2.12. Synthesis of 4-methoxyphenylisocyanide **(13)**

This procedure was adapted from Kamijo and co-workers.[34] To a solution of **12** (0.631 g, 4.17 mmol) in anhydrous THF (10 mL) was added distilled NEt_3 (3 mL, 14 mmol). The mixture was cooled on an ice bath, $POCl_3$ (0.6 mL, 5.7 mmol) was added with a syringe, and it was stirred for 1 h. 150 mL of aqueous saturated $NaHCO_3$ was added, and the mixture was extracted once with ether. The organic layer was washed four times with ether, dried over $MgSO_4$ and concentrated under reduced pressure to yield **13** as a black solid with an intense, sweet smell in 59% yield (0.328, 2.46 mmol).

^{1}H-NMR (400 MHz, $CDCl_3$): δ (ppm) 7.20 (d, J = 8.8 Hz, 2H), 6.77 (d, J = 8.8 Hz, 2H), 3.72 (s, 3H). ^{13}C-NMR (101 MHz, $CDCl_3$): δ (ppm) 162.59 (t, J = 5 Hz), 159.86, 127.71, 119.42 (t, J = 14 Hz), 114.55, 55.57.

6.2.13. Synthesis of 2,6-di(imino-4-phenyl)-pyridine derivatives

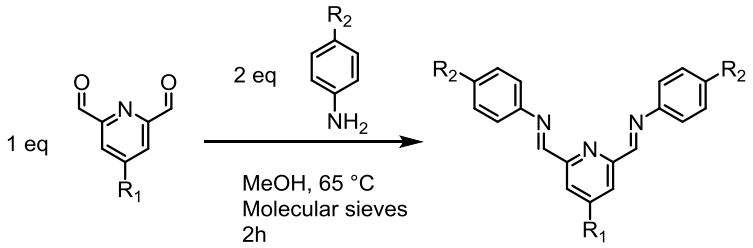

Figure 35: Synthesis of 2,6-di(imino-4-phenyl)-pyridine derivatives. R_1=H, $OC_{12}H_{25}$, R_2=OCH_3, $OC_{12}H_{25}$, $O(–CH_2CH_2–)_3OCH_3$ (TEG)

This procedure was adapted from Reedijk and co-wokers[36] and is general for the synthesis of all 2,6-diiminophenylpyridine pincer ligands, shown in Figure 35. In a round-bottomed flask, 1 equivalent of a 2,6-pyridinedicarbalehyde and 2 equivalents of an aniline were dissolved in anhydrous MeOH taken from a glovebox under Ar(g). The solution or suspension was stirred under reflux for 2h over molecular sieves and then further dispersed in anhydrous DCM. Molecular sieves were removed either by filtration or decantation. The filtrate was evaporated to yield 2,6-di(imino-4-phenyl)-pyridine derivatives.

6.2.14. Synthesis of 2,6-di(imino-4-methoxyphenyl)pyridine (diMIPPy)

diMIPPy (R_1=H, R_2=OCH_3) was obtained as yellow crystals from 2,6-pyridinedicarbaldehyde (0.1000 g, 0.740 mmol) and 4-methoxyaniline (0.1823 g, 1.480 mmol) and purified by filtration of a DCM solution. Yield: 43% (0.1108 g, 0.321 mmol).

^{1}H-NMR (400 MHz, CD_3CN): δ (ppm) 8.67 (s, 2H), 8.23 (d, J = 7.8 Hz, 2H), 7.99 (t, J = 7.8 Hz, 1H), 7.39 (d, J = 8.9 Hz, 4H), 7.00 (d, J = 8.9 Hz, 4H), 3.83 (s, 6H). ^{13}C-NMR (101 MHz, CD_3CN): δ (ppm) 158.86, 157.45, 154.73, 143.07, 137.25, 122.52, 121.89, 114.12, 54.87.

6.2.15.Synthesis of 2,6-di(imino-4-dodecyloxyphenyl)pyridine (diDoIPPy)

diDoIPPy (R_1=H, R_2=$OC_{12}H_{25}$) was obtained as a yellow powder from 2,6-pyridindicarbaldehyde (0.0365 g, 0.270 mmol) and 4-dodecyloxyaniline (**6**) (0.150 g, 0.541 mmol) and purified by filtration of a DCM dispersion of the reaction mixture. Yield: unknown.

^{1}H-NMR (400 MHz, $CDCl_3$): δ (ppm) 8.71 (s, 2H), 8.25 (d, J = 10.7 Hz, 2H), 7.91 (t, J = 7.5 Hz, 1H), 7.35 (d, J = 8.7 Hz, 4H), 6.95 (d, J = 8.8 Hz, 4H), 3.99 (t, J = 6.6 Hz, 4H), 1.80 (p, J = 7.4 Hz, 4H), 1.53 – 1.41 (m, 4H), 1.34 (b, 32H), 0.88 (t, J = 6.9 Hz, 6H). ^{13}C-NMR (101 MHz, $CDCl_3$)): δ (ppm) 158.69, 157.55, 154.88, 143.30, 137.15, 122.76, 122.66, 115.01, 77.32, 77.00, 76.68, 68.29, 31.92, 29.66, 29.63, 29.60, 29.58, 29.40, 29.35, 29.28, 26.05, 22.69, 14.12. MS (ESI): Expected 654.4993 for $[M+H]^+$, found 654.4981.

6.2.16.Synthesis of 2,6-di(imino-4-methoxytri(ethylene glycol)phenyl)pyridine (diTegIPPy)

diTegIPPy (R_1=H, R_2=$O(–CH_2CH_2–)_3OCH_3$) was obtained as a yellow wax from 2,6-pyridinedicarbaldehyde (0.0403 g, 0.2983 mmol) and 4-methoxytri(ethylene glycol) (**10**) (0.1523 g, 0.5965 mmol) without purification. Yield: 92% (0.168 g, 0.2756 mmol).

^{1}H-NMR (400 MHz, $CDCl_3$): δ (ppm) 8.70 (s, 2H), 8.25 (d, J = 7.8 Hz, 2H), 7.91 (t, J = 7.8 Hz, 1H), 7.35 (d, J = 8.9 Hz, 4H), 6.98 (d, J = 8.8 Hz, 4H), 4.17 (t, J = 5.2 Hz, 4H), 3.88 (t, J = 5.2 Hz, 4H), 3.78 – 3.73 (m, 4H), 3.72 – 3.65 (m, 8H), 3.59 – 3.54 (m, 4H), 3.39 (s, 6H).

6.2.17.Synthesis of 4-dodecyloxy-di(imino-4-methoxytri(ethylene glycol)phenyl)-pyridine (diTegIPDoPy)

diTegIPDoPy was obtained from 4-dodecyloxy-2,6-pyridinedicarbaldehyde (**4**) (0.0956 g, 0.2992 mmol) and 4-methoxytri(ethylene glycol)-aniline (**10**) (0.1528 g, 0.5985 mmol) as a brown wax without purification. Yield: At least 40% (0.094 mg, 0.1184 mmol).

^{1}H-NMR (400 MHz, $CDCl_3$): δ (ppm) 8.64 (s, 2H), 7.76 (s, 2H), 7.33 (d, *J* = 8.4 Hz, 4H), 6.97 (d, *J* = 8.4 Hz, 4H), 4.17 (s, 6H), 3.88 (s, 4H), 3.76 (s, 4H), 3.68 (s, 8H), 3.56 (s, 4H), 3.49 (s, 4H), 3.38 (s, 6H), 1.85 (s, 2H), 1.49 (s, 2H), 1.27 (s, 16H), 0.88 (s, 3H). All peaks were broad.

6.2.18. Synthesis of 4-dodecyloxy-di(iminio-4-dodecyloxyphenyl)pyridine (diDoIPDoPy)

diDoIPDoPy was obtained from 4-dodecyloxy-2,6-pyridinedicarbaldehyde (**4**) (0.0864 g, 0.270 mmol) and 4-dodecyloxyaniline (**6**) (0.150 g, 0.541 mmol) a brown/red wax without purification. Yield: unknown.

^{1}H-NMR (400 MHz, C_6D_6): δ (ppm) 8.99 (s, 2H), 8.19 (s, 2H), 7.36 (d, *J* = 7.7 Hz, 6H), 6.84 (d, *J* = 8.4 Hz, 6H), 3.70 – 3.59 (m, 8H), 1.74 – 1.57 (m, 8H), 1.58 – 1.44 (m, 5H), 1.31 (s, 79H), 0.92 (t, *J* = 6.6 Hz, 15H). The multiplicities and integrals do not match well to the expected features.

6.2.19.Synthesis of palladium-2,6-di(imino-4-phenyl)-pyridine ditetrafluoro-borate salt (Pd-diMIPPy)

This procedure was adapted from Nitschke and co-workers.[21] To a solution of $Pd(NCCH_3)_4(BF_4)_2$ (50 mg, 0.1126 mmol) in distilled acetonitrile (1 mL) was added a solution of diMIPPy (38.8 mg, 0.1126 mmol) in distilled acetonitrile (23 mL) in an oven-dried flask. The intensely red solution was stirred for 22h at 50 °C over molecular sieves, after which it was concentrated under reduced pressure to give Pd-diMIPPy as a red solid. It was further purified by dissolution in a minimum volume of acetonitrile and precipitation by ether. Yield: 85% (63.8 mg, 0.096 mmol).

^{1}H NMR (400 MHz, CD_3CN) δ (ppm): 8.48 (t, *J* = 8.1 Hz, 1H), 8.20 (s, 2H), 8.12 (d, *J* = 8.0 Hz, 2H), 7.49 (d, *J* = 8.8 Hz, 4H), 7.10 (d, *J* = 8.7 Hz, 4H), 3.88 (s, 6H).

6.2.20.Synthesis of chloroplatinum-2,6-di(imino-4-phenyl)-pyridine monotetrafluoro-borate salt (Cl-Pt-diMIPPy)

To a dispersion of diMIPPy (38.5 mg, 0.111 mmol) in distilled acetonitrile in an oven-dried flask was added $AgBF_4$ (21.7 mg, 0.111 mmol) stored in a glovebox under Ar(g) atmosphere and $PtCl_2(NCCH_3)_2$ (0.0388 g, 0.111 mmol). The flask was fitted with a reflux condenser and the deep yellow solution was stirred for 20 h over molecular sieves. The mixture was filtrated over Celite on a glass filter to remove AgCl, and the solution was concentrated to 1 mL. Cl-Pt-diMIPPy was precipitated by addition of diethyl ether, which was decanted. The brown solid was further washed with ether to give Cl-Pt-diMIPPy. Yield: 90% (66 mg, 0.0944 mmol).

^{1}H-NMR (400 MHz, CD_3CN) δ (ppm): 8.79 (s, 2H), 8.24 (t, *J* = 7.5 Hz, 1H), 7.97 (d, *J* = 7.7 Hz, 2H), 7.20 (d, *J* = 8.8 Hz, 4H), 6.81 (d, *J* = 8.9 Hz, 3H), 3.76 (s, 6H), 2.58 – 2.52 (m, 0.6H), 2.50 – 2.45 (m, 17H). ^{13}C-NMR (101 MHz, CD_3CN) δ (ppm): 159.48, 154.31, 150.35, 140.96, 139.88, 128.71, 122.99, 114.09, 54.89, 2.87. Low-resolution MS (ESI): Expected: 575 for $[M\text{-}BF_4]^+$, found: 576.

6.2.21.Synthesis of chloroplatinum-4-dodecyloxy-2,6-di(imino-4-methoxytri(ethylene glycol)phenyl)-pyridine monotetrafluoro-borate salt (Cl-Pt-diTegIPDoPy)

To $PtCl_2(NCCH_3)_2$ (0.0438 g, 0.1259 mmol) and $AgBF_4$ (0.0245 g, 0.1259 mmol) in an oven-dried flask was added a dispersion of diTegIPDOPy (0.094 g, 0.1184 mmol) in distilled acetonitrile. The dispersion was stirred for 20h at 50 °C over molecular sieves, decanted, and concentrated under reduced pressure to give a crude mixture Cl-Pt-diTegIPDoPy, AgCl and unknown compounds. It was not purified. Yield: Unknown.

^{1}H-NMR (400 MHz, CD_3CN) δ (ppm): 8.68 (s, 2H), 7.45 (s, 2H), 7.27 (d, *J* = 8.5 Hz, 4H), 6.88 (d, *J* = 9.1 Hz, 4H), 4.24 (s, 3H), 4.08 (s, 4H), 3.76 (s, 4H), 3.65 – 3.49 (m, 12H), 3.45 (s, 4H), 3.27 (s, 6H), 2.53 (s, 3H), 2.47 (s, 7H), 1.51 (s, 2H), 1.30 (d, *J* = 15.9 Hz, 22H), 0.87 (s, 4H).

6.2.22.Synthesis of platinum-2,6-di(imino-4-methoxytri(ethylene glycol)phenyl)-pyridine ditetrafluoroborate salt (Pt-diTegIPPy)

diTegIPPy (75.0 mg, 0.123 mmol), $PtCl_2(NCCH_3)_2$ (42.8 mg, 0.123 mmol) and $AgBF_4$ (47.9 mg, 0.246 mmol) were dissolved in 15 mL of distilled acetonitrile. The solution was stirred for 20h at 60 °C over molecular sieves. The suspension was filtrated over Celite on a glass filter and concentrated. A red solid was precipitated by addition of diethyl ether to a minimum solution of the crude in acetonitrile. It was sonicated twice with diethyl ether, which was subsequently decanted. The solid was dried under reduced pressure. Yield: Above 63% (80 mg, 0.079 mmol).

^{1}H-NMR (400 MHz, CD_3CN) δ (ppm): 10.06 (s, 0.3H), 8.84 (s, 2H), 8.26 (t, *J* = 7.6 Hz, 1H), 7.96 (d, *J* = 7.7 Hz, 2H), 7.44 (d, *J* = 8.4 Hz, 5H), 6.98 (d, *J* = 8.8 Hz, 6H), 4.13 (s, 8H), 3.83 – 3.73 (m, 9H), 3.66 – 3.42 (m, 36H), 3.29 (s, 13H), 2.67 – 2.58 (m, 8H). Due to hydrolysis, there are far more peaks than protons for the product.

6.2.23.Multicomponent synthesis of pyridine-platinum complex of 2,6-di(imino-4-methoxyphenyl)pyridine (pyridine-Pt-diMIPPy)

2,6-pyridinedicarbaldehyde (15 mg, 0.111 mmol), 4-methoxyaniline (27.3 mg, 0.222 mmol), pyridine (8.94 µL, 0.111 mmol), $PtCl_2(NCCH_3)_2$ (38.6 mg, 0.111 mmol) and $AgBF_4$ (43.2 mg, 0.222 mmol) were dissolved in distilled acetonitrile and stirred for 48 h at 65 °C over molecular sieves. The green suspension was filtrated over Celite on glass and the filtrate was concentrated under reduced pressure. Pyridine-Pt-diMIPPy (26.2 mg, 0.0032 mmol) was precipitated out of a 1 mL acetonitrile solution with diethyl ether. Yield: 29%.

^{1}H-NMR (400 MHz, CD_3CN) δ (ppm): 8.78 (s, 2H), 8.73 – 8.53 (m, 1H), 8.23 (t, *J* = 7.7 Hz, 1H), 7.95 (d, *J* = 7.7 Hz, 2H), 7.59 – 7.38 (m, 2H), 7.22 (d, *J* = 8.9 Hz, 4H), 6.82 (d, *J* = 8.9 Hz, 4H), 3.76 (s, 6H), 2.50 (s, 0.6H), 2.47 (s, 0.7H), 2.38 (s, 0.5H).

6.2.24. Synthesis of 4-picoline-platinum complex of 2,6-di(imino-4-methoxyphenyl)pyridine (pyridine-Pt-diMIPPy) by exchange with the pyridine complex

Pyridine-Pt-diMIPPy (3.6 mg, 4.7 µmol) and a 1 M solution 4-picoline in CD_3CN (5.8 µL, 5.8 µmol) were transferred into an NMR tube and stirred at 60 °C for 20 h.

6.2.25. Attempt at synthesis of 4-methoxyisocyanide platinum complex and 2,6-di(imino-4-methoxyphenyl)pyridine (4-methoxyphenylisocyanide-Pt-diMIPPy)

Cl-Pt-diMIPPy (16.8 mg, 0.025 mmol), 4-methoxyphenylisocyanide (10.3 mg, 0.076 mmol) and $AgBF_4$ (4.9 mg, 0.025 mmol) were dissolved in 5 mL of anhydrous MeOH and stirred for 20 h at RT. The suspension was filtrated over Celite on glass and the filtrate was concentrated under reduced pressure. A brown solid was precipitated with diethyl ether out of a 1 mL acetonitrile solution of the crude. Recovery: 26.6 mg.

6.2.26. Attempt at synthesis of 4-methoxytri(ethylene glycol) platinum complex of diTegIPPy (4-Teg-pyridine-Pt-diTegIPPy)

Pt-diTegIPPy (80.0 mg, 0.0786 mmol) and 4-methoxytri(ethylene glycol)pyridine were dissolved in anhydrous MeOH in an oven-dried flask and stirred for 3 h at 40 °C over molecular sieves. A suspension of the crude in anhydrous MeOH was filtrated twice over Celite on a glass filter. A sticky tar was precipitated by addition of diethyl ether to a minimum solution of the crude in anhydrous MeOH.

6.2.27. Attempt at synthesis of 4-methoxytri(ethylene glycol) platinum complex of diMIPPy (4-TEG-pyridine-Pt-diTegIPPy)

Cl-Pt-diMIPPy (16.3 mg, 0.0246 mmol), 4-TEG-pyridine (5.9 mg, 0.0246 mmol) and $AgBF_4$ (4.8 mg, 0.00246 mmol) were dissolved in a 1:1 mixture of anhydrous MeOH and anhydrous DCM. The green solution was stirred for 3 d at 40 °C in the presence of molecular sieves. A suspension of the crude in anhydrous MeOH was filtrated over Celite on a glass filter. The filtrate was concentrated to give a sticky solid, which was impure, uncoordinated diMIPPy and free 4-TEG-pyridine.

Bibliography

1. Lehn, J.-M. From supramolecular chemistry towards constitutional dynamic chemistry and adaptive chemistry. *Chem. Soc. Rev.* **36,** 151–60 (2007).

2. Whitesides, G. M., Mathias, J. P. & Seto, C. T. Molecular Self-Assembly and Nanochemistry: A Chemical Strategy for the Synthesis of Nanostructures. *Science* **254,** 1312–1319 (1991).

3. Lindsey, J. S. Self-assembly in synthetic routes to molecular devices. Biological and chemical perspectives: A review. *New J. Chem.* 153–180 (1991).

4. Rowan, S. J., Cantrill, S. J., Cousins, G. R. L., Sanders, J. K. M. & Stoddart, J. F. Dynamic covalent chemistry. *Angew. Chemie Int. Ed. Engl* **41,** 898–952 (2002).

5. Bull, S. D. *et al.* Exploiting the Reversible Covalent Bonding of Boronic Acids: Recognition, Sensing, and Assembly. *Acc. Chem. Res.* **46,** 312–326 (2013).

6. Meyer, C. D., Joiner, C. S. & Stoddart, J. F. Template-directed synthesis employing reversible imine bond formation. *Chem. Soc. Rev.* **36,** 1697–1844 (2007).

7. Schultz, D. & Nitschke, J. R. Dynamic covalent and supramolecular direction of the synthesis and reassembly of copper (I) complexes. *Proc. Natl. Acad. Sci. U. S. A.* **102,** 11191–11195 (2005).

8. Matharu, Z., Bandodkar, A. J., Gupta, V. & Malhotra, B. D. Fundamentals and application of ordered molecular assemblies to affinity biosensing. *Chem. Soc. Rev.* **41,** 1363–1402 (2012).

9. Mauro, M., Aliprandi, A., Septiadi, D., Kehr, N. S. & De Cola, L. When self-assembly meets biology: luminescent platinum complexes for imaging applications. *Chem. Soc. Rev.* **43,** 4144–4166 (2014).

10. Zhang, J., Li, S. & Li, X. Polymeric Nano-Assemblies as Emerging Delivery Carriers for Therapeutic Applications: A Review of Recent Patents Jianxiang. *Recent Pat. Nanotechnol.* **3,** 225–231 (2009).

11. Chen, L., Chen, Q., Wu, M., Jiang, F. & Hong, M. Controllable Coordination-Driven Self-Assembly : From Discrete Metallocages to Infinite Cage-Based Frameworks. *Acc. Chem. Res.* **48,** 201–210 (2015).

12. Cook, T. & Stang, P. Coordination-Driven Supramolecular Macromolecules via the Directional Bonding Approach. *Adv. Polym. Sci.* **261,** 229–248 (2013).

13. Katsuki, T. Unique asymmetric catalysis of cis-b metal complexes of salen and its related Schiff-base ligands. *Chem. Soc. Rev.* **33,** 437–444 (2004).

14. Chou, P.-T., Chi, Y., Chung, M.-W. & Lin, C.-C. Harvesting luminescence via harnessing the photophysical properties of transition metal complexes. *Coord. Chem. Rev.* **255,** 2653–2665 (2011).

15. Liang, B., Tong, R., Wang, Z., Guo, S. & Xia, H. High intensity focused ultrasound responsive metallo-supramolecular block copolymer micelles. *Langmuir* **30,** 9524–9532 (2014).

16. Po, C. & Wing-Wah Yam, V. A metallo-amphiphile with unusual memory behaviour: effect of temperature and structure on the self-assembly of triethylene glycol (TEG)–pendant platinum(II) bzimpy complexes. *Chem. Sci.* **5,** 4868–4872 (2014).

17. Allampally, N. K., Strassert, C. a. & De Cola, L. Luminescent gels by self-assembling platinum complexes. *Dalt. Trans.* **41,** 13132–13137 (2012).

18. Strassert, C. A. *et al.* Switching on luminescence by the self-assembly of a platinum(II) complex into gelating nanofibers and electroluminescent films. *Angew. Chemie Int. Ed. Engl* **50,** 946–950 (2011).

19. Xiao, X.-S., Lu, W. & Che, C.-M. Phosphorescent nematic hydrogels and chromonic mesophases driven by intra- and intermolecular interactions of bridged dinuclear cyclometalated platinum(ii) complexes. *Chem. Sci.* **5,** 2482–2488 (2014).

20. Koo, C.-K. *et al.* A Triphenylphosphonium-Functionalised Cyclometalated Platinum(II) Complex as a Nucleolus-Specific Two-Photon Molecular Dye. *Chem. - A Eur. J.* **16,** 3942–3950 (2010).

21. Browne, C., Ronson, T. K. & Nitschke, J. R. Palladium-Templated Subcomponent Self-Assembly of Macrocycles, Catenanes, and Rotaxanes. *Angew. Chemie Int. Ed. Engl* **53,** 10701–10705 (2014).

22. Ingham, C. J., ter Maat, J. & de Vos, W. M. Where bio meets nano: the many uses for nanoporous aluminum oxide in biotechnology. *Biotechnol. Adv.* **30,** 1089–1099 (2012).

23. Miskowski, V. & Houlding, V. Electronic Spectra and Photophysics of Platinum(II) Complexes with a-Diimine Ligands. Solid-state Effects. 2. Metal-Metal Interaction in Double Salts and Linear Chains. *Inorg. Chem.* **30,** 4446–4452 (1991).

24. Houlding, V. H., Miskowskib, V. M., Technology, B. & Interlocken, C. The effect of linear chain structure on the electronic structure of Pt(II) diimine complexes. *Coord. Chem. Rev.* **111,** 145–152 (1991).

25. Busto, E., González-Álvarez, A., Gotor-Fernández, V., Alfonso, I. & Gotor, V. Optically active macrocyclic hexaazapyridinophanes decorated at the periphery: synthesis and applications in the NMR enantiodiscrimination of carboxylic acids. *Tetrahedron* **66,** 6070–6077 (2010).

26. Kim, M., Euler, W. B. & Rosen, W. LFER Correlation of 13 C Chemical Shift in Para-Substituted Phenyl Isocyanide : Implications for Formation of a Unique Polymer. *J. Org. Chem.* **62,** 3766–3769 (1997).

27. Maeda, C. *et al.* Selective formation of a single atropisomer of meso-meso-linked Zn(II) diporphyrin through supramolecular self-assembly. *Chem. - A Eur. J.* **15,** 9681–9684 (2009).

28. Lu, W., Chen, Y., Roy, V. a L., Chui, S. S.-Y. & Che, C.-M. Supramolecular polymers and chromonic mesophases self-organized from phosphorescent cationic organoplatinum(II) complexes in water. *Angew. Chemie Int. Ed. Engl* **48,** 7621–7625 (2009).

29. Hosseini-Sarvari, M. & Sharghi, H. ZnO as a New Catalyst for N-Formylation of Amines under Solvent-Free Conditions. *J. Org. Chem.* **71,** 6652–6654 (2006).

30. Temussi, P. A., Tancredi, T. & Quadrifoglio, F. Conformational Rigidity of the Amide Bond. A Variable-Temperature Nuclear Magnetic Resonance Study of the System Ag+-N,N-Dimethylacetamide. *J. Phys. Chem.* **73,** 4227–4232 (1969).

31. Phillips, W. D. Restricted Rotation in Amides as Evidenced by Nuclear Magnetic Resonance. *J. Chem. Phys.* **23,** 1363–1364 (1955).

32. Bourns, A. J. R., Gillies, D. G. & Randall, E. W. Cis-trans isomerism in formanilide. *Tetrahedron* **20,** 1811–1818 (1964).

33. Gim, H. J., Kang, B. & Jeon, R. Synthesis and Biological Activity of 5-{4-[2-(Methyl-p-substi- tuted phenylamino)ethoxy] benzyl}thiazolidine-2,4-diones. *Arch. Pharm. Res.* **30,** 1055–1061 (2007).

34. Kamijo, S., Jin, T., Yamamoto, Y., Si, C. & Si, S. Cyanamide Synthesis by the Palladium-Catalyzed Cleavage of a Si-N Bond. *Angew. Chemie Int. Ed. Engl* **114,** 1858–1860 (2002).

35. Nelson, S. M., Lavery, A. & Drew, M. G. B. Copper(I) Schiff-base Complexes: Reversible Carbon Monoxide Binding, Reactions with Dioxygen, and the Structure of a Dinuclear Complex containing Co-ordinated and Unco-ordinated Alkene Groups. *J. Chem. Soc. Dalt. Trans.* 911–920 (1986).

36. Garza-Ortiz, A., Maheswari, P. U., Siegler, M., Spek, A. L. & Reedijk, J. Ruthenium(III) chloride complex with a tridentate bis(arylimino)pyridine ligand: synthesis, spectra, X-ray structure, 9-ethylguanine binding pattern, and in vitro cytotoxicity. *Inorg. Chem.* **47,** 6964–6973 (2008).

37. Gibson, V. C., Redshaw, C. & Solan, G. A. Bis(imino)pyridines: Surprisingly Reactive Ligands and a Gateway to New Families of Catalysts. *Chem. Rev.* **107,** 1745–1776 (2007).

38. Lavery, A. & Nelson, S. M. Dinuclear Mono-μ-chloro-pyridyldiaza Rhodium(I) Complexes derived from Pyridyldi-imines via hydrogen transfer from Ethanol. *J. Chem. Soc. Dalt. Trans.* 1053–1055 (1985).

39. Webba, M. da S. *et al.* Stereochemically non-rigid transition metal complexes of 2, 6-bis[1-(phenylimino)ethyl]pyridine(BIP). Part 3 .Dynamic NMR studies of fac-[PtXMe3(BIP)] (X=C1, Br, or I). Crystal structure of fac-[PtIMe3(BIP)]. *J. Organomet. Chem.* **555,** 35–47 (1998).

40. Lavery, A. & Nelson, S. M. Dinuclear Intermediates in the Oxidation of Pendant Olefinic Groups of Palladium(II)-coord inated Schiff-base Ligands. *J. Chem. Soc. Dalt. Trans.* 615–620 (1984).

41. Liu, P., Yan, M. & He, R. Bis(imino)pyridine palladium(II) complexes as efficient catalysts for the Suzuki-Miyaura reaction in water. *Appl. Organomet. Chem.* **24,** 131–134 (2009).

42. Groen, J. *et al.* Insertion Reactions into Palladium-Carbon Bonds of Complexes Containing Terdentate Nitrogen Ligands; Experimental and Ab initio MO Studies. *Eur. J. Inorg. Chem.* 1129–1143 (1998).

43. Liu, P., Zhou, L., Li, X. & He, R. Bis(imino)pyridine palladium(II) complexes: Synthesis, structure and catalytic activity. *J. Organomet. Chem.* **694,** 2290–2294 (2009).

44. Xing, L.-B. *et al.* Reversible multistimuli-responsive vesicles formed by an amphiphilic cationic platinum(II) terpyridyl complex with a ferrocene unit in water. *Chem. Commun.* **48,** 10886–10888 (2012).

45. Habata, Y. *et al.* Argentivorous Molecules: Structural Evidence for Ag+ - π Interactions in Solution. *Org. Lett.* **14,** 4576–4579 (2012).

46. Young, A. G. & Hanton, L. R. Square planar silver(I) complexes: A rare but increasingly observed stereochemistry for silver(I). *Coord. Chem. Rev.* **252,** 1346–1386 (2008).

47. Di Bernardo, P., Melchior, a., Portanova, R., Tolazzi, M. & Zanonato, P. L. Complex formation of N-donor ligands with group 11 monovalent ions. *Coord. Chem. Rev.* **252,** 1270–1285 (2008).

48. Mauro, M. *et al.* Self-assembly of a neutral platinum(II) complex into highly emitting microcrystalline fibers through metallophilic interactions. *Chem. Commun.* **50,** 7269–7272 (2014).

49. Bacchi, A. *et al.* Reactions of the homoleptic acetonitrile complexes of palladium and platinum with diethylamine. *Inorganica Chim. Acta* **363,** 2467–2473 (2010).

50. Ito, M. *et al.* A novel method for creation of free volume in a one-component self-assembled monolayer. Dramatic size effect of para-carborane. *J. Mater. Chem.* **15,** 478–483 (2005).